Metabolic properties of the hyperthermophilic sulfate reducing archaea of the genus *Archaeoglobus* in deep-sea hydrothermal vent systems

Hannah Rose Babel

Master's Thesis

K.G. Jepsen Center for Deep Sea Research

Department of Biological Sciences

University of Bergen, Norway

June 2019

List of Abbreviations

AMOR Arctic Mid-Ocean Ridge

AMP adenosine monophosphate

Apr adenylyl-sulfate reductase

APS adenosine-5'-phophosulfate

ATP adenosine triphosphate

Bp base pairs

CD circular dichroism

CDNN CD Spectra Deconvolution version 2.1

CPM counts per minute

Da (KDa) Dalton (kilodalton)

DMSO dimethyl sulfoxide

DNA Deoxyribonucleic acid

DSR dissimilatory sulfate reduction

Dsr dissimilatory sulfite reductase

g/mg/kg/µg grams/ milligrams/ kilograms / nanograms/ micrograms

HEPES

4-(2-hydroxyethyl)-1-piperazineethanesulfonic acid

IMAC immobilized metal affinity chromatography

IPTG isopropyl β-D-1 thiogalactopyranoside

Kb kilobases

LB Lysogeny broth

LCVF Loki's Castle Vent Field

LDH Lactate Dehydrogenase

L/ml/µl liter, milliliter, microliter

Mbq Magebecquerel

MOPS 3-(*N*-morpholino)propanesulfonic acid

NAD+ Oxidized Nicotinamide Adenine Dinucleotide (NAD)

NADH Reduced Nicotinamide Adenine Dinucleotide (NAD)

NCBI National Center for Biotechnology Information

NEB New England BioLabs

OD Optical Density

ORF Open Reading Frame

OTU Operational Taxonomic Unit

PCR Polymerase Chain Reaction

Qmo oxidoreductase

RPM Rotations Per Minute

Sat ATP sulfurylase

SDS-PAGE sodium dodecyl sulfate-polyacrylamide gel electrophoresis

SOC Super Optimal Broth

SOM Sulfur oxidizing microorganisms

SRP sulfur reducing prokaryotes

SRR sulfate reduction rates

TAE Tris base, acetic acid and EDTA

TAG Trans-Atlantic Geotraverse

UTC Coordinated Universal Time

Abstract

Along the mid-ocean ridge system, super-heated fluids rich in metal sulfides expel out of the ocean floor, precipitating sulfides and forming black smoker chimneys. The precipitated sulfide forms the chimney wall and the fluids abundant in reductive minerals provide the structure, shelter, and energy sources needed for chemosynthetic primary production. The fluids of up to 350 °C and the seawater of -2 °C form a steep temperature gradient within the wall. Likewise, the composition of the hydrothermal vent fluids versus the seawater form steep nutrient and oxygen gradients for different niches of microbes to live, including sulfate reducing prokaryotes (SRPs). In the first part of this study, the rates of sulfate reduction from hydrothermal vents samples were measured to quantify the role of these organisms in their ecosystem. One type of SRP is the hyperthermophilic sulfate reducing archaea from the genus *Archaeoglobus.* These organisms reduce sulfate, as well as thiosulfate and sulfite, into hydrogen sulfide through the dissimilatory sulfate reduction (DSR) pathway. Proteins from a putative lactate dehydrogenase from *Archaeoglobus fulgidus* previously hypothesized to be an electron supply needed for the second step of the DSR pathway were further researched in the second part of this study. Minute amounts of sulfate reduction was measured within the chimney wall of a black smoker located at Loki's Castle Vent Field (LCVF) and despite the correlating community analysis lacking evidence of the existence *Archaeoglobus,* the presence of the sulfate reducing bacteria *thermodesulfobacteriaceae* and *Desulfohalobiaceae* were found in low relative abundance. Genes encoding a putative lactate dehydrogenase (LDH) complex and other associated proteins from *Archaeoglobus fulgidus* were cloned into *E. coli*. This LDH complex may play an important role in providing electrons to the DSR pathway within *A. fulgidus*. Three of these proteins were successfully expressed and purified. Of the proteins purified, the glycolate oxidase subunit was tested for secondary structure and melting temperature using circular dichroism, which gave further evidence to the protein being a of hyperthermophilic nature.

Acknowledgements

I would like to thank all the members of the K.G. Jepsen Center for Deep Sea Research. Over the past year and a half they have endlessly provided me with encouragement, excitement for research, and a developing community. I feel honored to be a part of this research group. Secondly, I would like to thank my classmates who have gone through the Master's program with me as we helped to lift each other up when things got difficult. Particularly, I would like to thank Hasan Arsin for his endless help with cloning, and phenomenal mentorship in the lab. I would also like to extend thanks to Anita-Elin Fedøy and Francesca Vulcano for always being open to my questions and to show me the ropes in the lab as well as on the Research Cruise. Acknowledgements belong to Desiree Reordink for all her guidance and help with the Sulfate Reduction Rates.

I would not have been able to do this project without the support of my family encouraging me to follow my passions, even when they take me so far away. I love you and I hope to only ever make you proud.

Lastly, I would like to give my greatest thanks to my supervisor, Ida Helene Steen. Your endless encouragement and belief in me drove me to love my project most. Your passion for not only research, but teaching shone through and taught me to believe in myself and my research abilities. Thank you for your patience with me throughout this project, your positive attitude, and most of all being a supervisor I can look up to in so many ways.

This project was a very steep learning curve for me, and with that comes great trails, but even greater rewards. I never would have believed I would be study the deep sea, but I fully enjoyed the content of my project. It fascinated me and allowed me to obtain skills that I otherwise would have never had the opportunity. Thank you Ida for giving me a chance and letting me work on this project.

Hannah

Table of Contents

1.0 Introduction

When hydrothermal vent systems were discovered in 1977 by scientists from Woods Hole Oceanographic Institution (MA, USA), it opened an entire new door of research. Despite hypotheses of hydrothermal venting based on the geology found in ocean dredging and the temperature anomalies found in water samples, life in such extreme conditions was not known or expected to exist until the discoveries of life on deep-sea vents near the Galápagos Rift were published (Konhauser, 2009, Crane and Normark, 1977, Scott et al., 1974, Corliss et al., 1979, Lonsdale, 1977). The extreme temperature gradient made from the mixing of superheated hydrothermal fluids and cold seawater in addition to the influx of nutrients from the plumes, creates many different habitats for primary producers to thrive (Munn, 2011). Far below the depths of light, microorganisms found near "black smokers" rely on the chemical gradients formed by the flow of the solute-rich fluids into the seawater (Konhauser, 2009). Jannasch and Wirsen (1979) proposed that the microbial life in these systems was possible through chemosynthesis. While chemosynthesis can occur in many different ecosystems on the planet, it was found to be much stronger at hydrothermal vents (Jannasch and Wirsen, 1979). In chemosynthesis, the energy formed from the oxidation of the inorganic matter coming from the hydrothermal fluids is used to form organic carbon, creating the foundation for deep sea hydrothermal vent ecosystems. In the past forty years, knowledge about these systems has gone from the unseen mystery to actively sampled and mapped ecosystems.

1.1 Hydrothermal Vent Systems

As the seafloor spreads in the deep ocean and new ocean crust forms, seawater suffuses up to 8 kilometers into the earth and gradually becomes heated from the magma below (Kelley et al., 2002). The magnesium, sulfate, and bicarbonate found in the fluids are dissolved into the rock, causing the formation of acids that leach different elements and metals away from the rocks that then become incorporated into the fluids (Konhauser, 2009, Munn, 2011). With the downwelling of the seawater, the subsurface fluids become rich with copper, manganese, iron, zinc, silicic acid, hydrogen, calcium, hydrogen sulfide, carbon dioxide, and methane (Konhauser, 2009, Munn, 2011). The heated and pressurized fluids rise towards the ocean floor, precipitating

compounds, such as metal sulfides, and forming structures called chimneys (Munn, 2011). Plumes of the hot, metal-rich, buoyant hydrothermal fluids flow out through these chimneys and mix with the surrounding cold seawater (Konhauser, 2009). The chemical properties of the hydrothermal fluids are dictated by the temperature of the rock the fluids circulate through, the amount of fluids that have previously travelled through the same channel, and the composition of the host rock as the fluids cool and interact with the rock by exchanging elements(Kelley et al., 2001, Kelley et al., 2002). While originally thought to only happen along mid-ocean ridges where new crust is forming, venting can occur in slow-spreading regions with old crust formations, such as the Lost City Vent Field located on 1.5 million-year-old crust (Kelley et al., 2001). The venting location, host rock composition, and temperature of the hydrothermal fluids all impact the formation of chimneys. In the old crustal regions, carbonate chimneys are found, however at the mid-ocean ridges chimneys formed are classified as white or black smokers, based on the apparent color of the fluids expelled (Kelley et al., 2001, Kelley et al., 2002). Black smoker chimneys are formed from hydrothermal fluids that have been superheated up to 380 °C and are rich in sulfate particles and metal sulfides, causing the fluids to come out through chimneys like black smoke (Konhauser, 2009, Munn, 2011).

In basaltic rock, when temperatures reach above 150 °C, the rock will take up the magnesium from the fluids and lose the alkalis it contains. Once the temperature reaches between 350 and 550 °C, the rocks lose copper, zinc, iron, lead, sulfur, and silicon dioxide to the hydrothermal fluids (Kelley et al., 2002). Unlike the fast-spreading East Pacific Rise dominated by the formation of small chimneys, the mid-ocean ridges in the Atlantic Ocean are slower spreading, forming large sulfide mounds and towering chimneys (Van Dover, 1995). Chimney structure is determined by the composition of the vent fluid, and as the sulfide structures form from the precipitates coming from the fluid, steep temperature and oxygen gradients are made in the chimney walls. The composition of the chimney walls, as well as the diffusing fluid, provides necessary substrates and nutrients for life. The gradients formed allow for species of microorganisms ranging from mesophilic, aerobic heterotrophs to hyperthermophilic, strictly anaerobic chemoautotrophs to live. The microbes in these deep-sea ecosystems utilize the wide range of electron donors and acceptors available in order to survive, as well as the array of carbon sources. As the temperature gradient goes from the ambient seawater temperature of 2 °C outside the chimney to the 350 °C temperature of the plume fluid inside of the chimney, the

microbial community changes (**Figure 1)**. The oxygenic seawater is depleted of oxygen and nitrate as the temperature rises above 50 °C, shifting the community structure from aerobic, to facultative anaerobic, and finally to strictly anaerobic microbes. The aerobic microorganisms primarily use the nitrate and carbon dioxide in the seawater as their electron acceptor and carbon source respectively, and obtain their energy using reduced sulfur (Kelley et al., 2002). The anaerobic microorganisms found at deep-sea hydrothermal vents are supported by hydrogen sulfide as the primary electron donor in chemosynthesis, as well as elemental sulfur, thiosulfate, hydrogen gas, and methane. The anaerobic sulfur reducers and methanogens found in the oxygen depleted regions of the chimney wall utilize the hydrogen with carbon dioxide or elemental sulfur for anaerobic respiration (Baross et al., 1982).

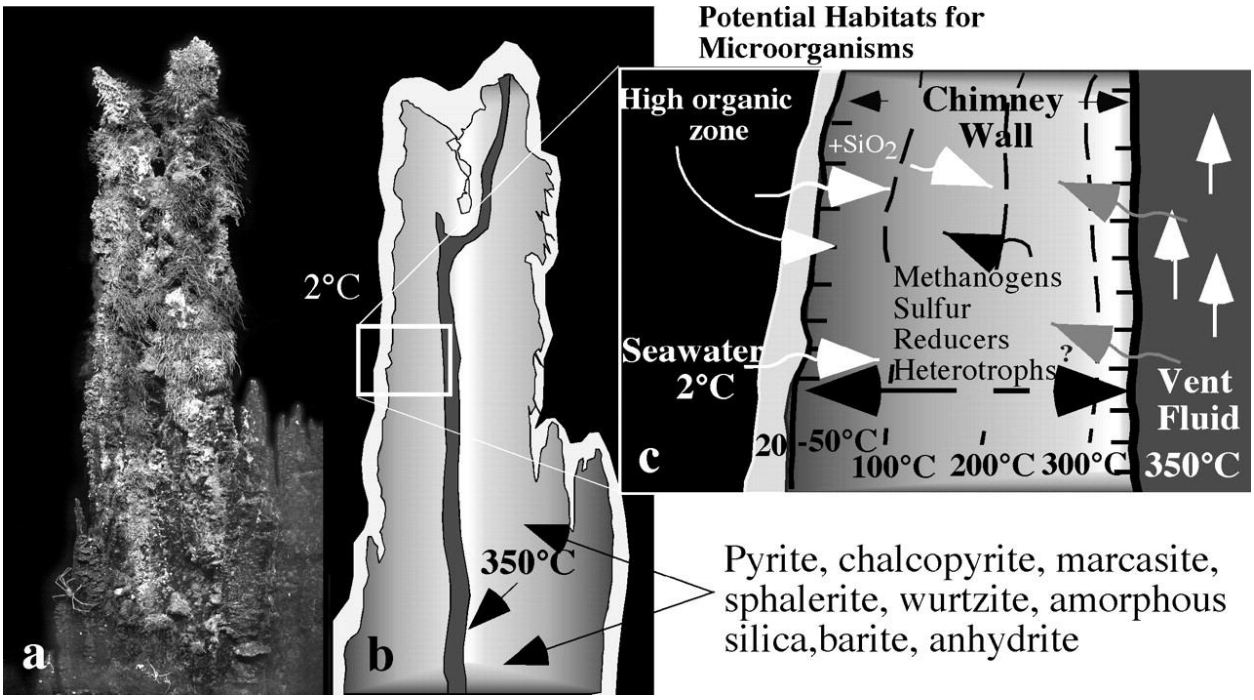

Figure 1 a.) an image of a black smoker chimney **b.)** the conceptual diagram of the cross-section of the photographed chimney and **c.)** the conceptual diagram of the chimney wall (figure by Kelley et al., 2002)

Furthermore, the number of microbial cells in the outer part of the chimney wall and higher on the chimney is greater than in inner and lower parts, increasing throughout the chimney wall with sulfide layers (Harmsen et al., 1997). The drastic temperature gradient and extreme temperatures

in the chimney wall is results in an environment only specialized organism can tolerate, making the outer and upper layers of a chimney a less limiting environment.

1.2 Loki's Castle Vent Field

Along the Arctic Mid Ocean Ridge (AMOR), a unique vent field, named Loki's Castle Vent Field (LCVF), was discovered in 2008 and comprised of four active black smoker chimneys atop two separate 20 to 30 meter sulfide mounds (Pedersen et al., 2010). The sulfide mounds located near a 30 km long axial vent ridge are comparable to the large Trans-Atlantic Geotraverse (TAG) mound found in 1985 at a slow spreading ridge (Pedersen et al., 2010; Rona et al., 1986). The black smoker chimneys and the sulfate and sulfide precipitation are characteristic of LCVF and other slow spreading ridges (Jaeschke et al., 2012). Here, microbial mats dominated by *Epsilonproteobacteria* grow densely on the chimneys and survive on the hydrothermal fluids rich in methane, ammonium, hydrogen, and hydrogen sulfides (ibid.). In this study, samples were taken from a black smoker found in LCVF, called Camel, to be analyzed to better understand the of energy metabolisms at this location and in deep-sea, black smoker, hydrothermal venting.

1.3 The Sulfur Cycle

The sulfur found in hydrothermal vents, leached from the basaltic host rock, is the basis for the microbial sulfur cycle in hydrothermal vent ecosystems. Sulfur is cycled in hydrothermal vent systems through processes of sulfur oxidation and reduction performed by primary producers. As the inorganic reduced sulfur is ejected from the plumes it is oxidized by sulfur-oxidizing microorganisms (SOM)s through sulfur oxidation pathways. This sulfur oxidation provides a source of sulfate for sulfate reducing prokaryotes found further inside the chimney. Of the SOMs found in black smoker chimney ecosystems, the dominating *Epsilonproteobacteria* found on microbial mats on the outside of the chimneys are capable of oxidizing sulfur, and therefore, act as a primary provider for the foundation for life for other microorganisms dependent on the

sulfur cycle by providing available oxidized sulfur to be reduced by sulfate reducing prokaryotes (SRP)s (Yamamoto and Takai, 2011).

Within the chimney wall and throughout the temperature gradient, SRPs from both bacterial and archaeal domains ranging from mesophilic to hyperthermophilic exist (Frank et al., 2013; Jaeschke et al., 2012; Nakagawa et al., 2004). The energy landscapes modelled by Dahle et al. (2015) found in modeling energy landscapes at LCVF, the abundance of SRPs increased with temperature, however never exceeding 7% of the relative abundance. Despite the relative low abundance to the community, the SRPs play an important role in reducing organic sulfur. SRPs can reduce sulfate and well as sulfur intermediates of the sulfur cycle, like thiosulfate and sulfite. Among the different mechanisms for sulfur reduction, the pathway highlighted in this study is the dissimilatory sulfate reduction pathway.

Sulfate reducing prokaryotes cycle sulfur by preforming anaerobic respiration through dissimilatory sulfate reduction (DSR) (Muyzer and Stams, 2008; Peck, 1961; Postgate, 1959). This is the process where sulfate (SO_4^{2-}) is reduced to sulfide through three steps. As a terminal electron acceptor in this process, sulfate is generally unfavorable due to the negativity of the reduction reaction. Therefore, it is necessary for the first step of DSR to be the formation of the more favorable adenosine-5'-phophosulfate (APS) and inorganic pyrophosphate through the activation of sulfate with adenosine triphosphate (ATP) by the enzyme ATP sulfurylase (*Sat*) (Muyzer & Stams, 2008; Peck, 1961). APS is then reduced to sulfite (SO_3^{2-}) through the enzyme adenylyl-sulfate reductase (*Apr*) with electrons donated from NADH or reduced ferredoxin, and then produces adenosine monophosphate (AMP) as an additional product of the reaction (Muyzer & Stams, 2008). The final step in DSR is the reduction of sulfite by dissimilatory sulfite reductase (*Dsr*) (**Figure 2**).

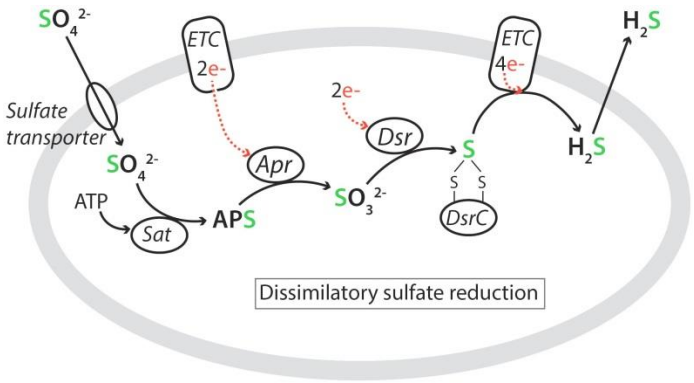

Figure 2 Simplified model of the dissimilatory sulfate reduction pathway from a review of the biogeochemical sulfur cycle by Jørgensen et al (2019).

1.4 The Genus *Archaeoglobus*

The most widely studied dissimilatory sulfate reducing prokaryotes, the most widely studied are found in the domain Bacteria and live under moderate environmental conditions (Pfennig et al., 1981; for a recent review see Rabus et al., 2015). However, the study of SRPs in the deep-sea hydrothermal vents is beneficial to broadening the understanding of sulfur cycling and the dissimilatory sulfate reduction pathway in extreme environments. The hyperthermophilic sulfate-reducing archaea of the genus *Archaeoglobus* are typically found in high-temperature habitats. Several species have been isolated and characterized including *A. fulgidus*, *A. profundus*, *A. veneficus*, *A. sulfaticallidus*, and *A. infectus* (Achenbach-Richter et al. 1987; Huber et al. 1997; Mori et al., 2008; Steinsbu et al., 2010; Stetter, 1988; von Jan et al., 2010). Of the isolated species, the model organism in hydrothermal vents from this genus is *A. fulgidus*. *A. fulgidus* was first isolated in Italy from a hydrothermal vent near Vulcano Island (Achenbach-Richter et al. 1987; Stetter, 1988). *A. fulgidus* can also utilize sulfite and thiosulfate as electron acceptors and the strain type VC-16 was found to use many carbon sources including; lactate, pyruvate, formate, ethanol, and carbon monoxide (Hocking et al., 2015; Klenk et al., 1998). In-depth studies, based on microarrays, of the energy metabolism of *A. fulgidus* were recently performed in the research group Deep-Sea Biology at BIO (Department of Biological Sciences, Bergen, Norway (Hocking et al., 2014; 2015)

1.5 Lactate Dehydrogenase

In previous studies on the metabolic pathways of *A. fulgidus*, it was hypothesized that putative lactate dehydrogenase (LDH) subunits form a complex and together with a lactate permease and a lactate dehydrogenase, perform lactate oxidation (Hocking et al., 2014). Lactate oxidation is a key coupled oxidation-reduction reaction the converts lactate to pyruvate coupled with the reduction of an electron carrier (**Equation 1**).

Equation 1 Lactate oxidation as performed by Lactate Dehydrogenase where NAD^+ and NADH are the representative electron carriers.

$$\text{Lactate} + NAD^+ \leftrightarrow \text{Pyruvate} + NADH$$

The lactate oxidation reaction is catalyzed through the lactate dehydrogenase enzymes. Depending on the form of lactate and the electron carriers used for the reaction within a cell, different lactate dehydrogenases are used. Reed and Hartzell (1999) discovered a lactate dehydrogenase encoded from the open reading frame (ORF) AF0394 in *A. fulgidus.* This lactate dehydrogenase used D-Lactate as both the carbon source and the electron source, with electrons then being carried through intermediate carrier proteins like quinones and cytochromes found in the cell membrane (Reed and Hartzell, 1999). In this study, they also identified other ORFs that were similar to other lactate dehydrogenases, despite lacking some components, such as AF0808 (ibid.). In more recent work by Hocking et al. (2014), AF0808 is instead hypothesized to be a subunit of a lactate dehydrogenase complex. The enzymes that catalyze the conversion of either L- or D-lactate to pyruvate are found in most living organisms with functions that vary from generating proton motive forces used for growth to NAD^+ formation, but certain types of these enzymes remain undefined in function for certain types (Garvie, 1980; Reed and Hartzell, 1999).

It was predicted that the putative LDH complex in *A. fulgidus* took part in energy conservation by potentially transferring electrons to a quinone-interacting, membrane-bound oxidoreductase (Qmo) complex and linking to the second step of DSR (Hocking et al., 2014). The Qmo complex consists of subunits A, B, and C (QmoABC) and has been suggested as a link between the electron transfer chain to *Apr*, providing the necessary energy input for DSR (Ramos et al., 2012). Revealing the structural organization of the LDH complex is important to understanding the role it plays in the electron flow in the cells and, furthermore, the role it has in the energy metabolism of *A. fulgidus.* Therefore, by testing for the heterologous production of soluble

subunits of the protein in *Escherichia coli*, an important step forward to revealing the structural organization of LDH is taken.

1.6 Aims of Study

The primary aim of this study was to deepen the understanding of the role that the genus *Archaeoglobus* have in deep-sea hydrothermal vent ecosystems as dissimilatory sulfate reducing prokaryotes. Using a range of methods in biochemistry, cultivations, and geochemistry, this role was explored.

In the first part of this two-part study, the focus was on the estimated rate of sulfate reduction in chimney material from a black smoker chimney from LCVF. This was used to estimate the amount of electron donors available in the ecosystem that can be recycled with sulfate being used as an electron acceptor. This part consisted of field work via participation on the KG Jepsen Research cruise to the AMOR vent fields in 2018 for sample collection for enrichment cultures, community analyses, and measuring sulfate reduction rates.

The second part of this study was aimed towards testing the ability to heterologously express and purify soluble components of the putative LDH complex and its related proteins from *A. fulgidus*¸ comprising of the ORFs AF0806-AF0812, for future functional characterization.

2.0 Methods

2.1 Sampling

Chimney samples were collected using *Æ*gir 6000 on ROV dive 22 aboard G.O. Sars 218, on July 16th, 2018 at 21:12 UTC. The samples were collected from the hydrothermal vent chimney, Camel, located at LCVF (73,5667° N, 8,1567° E) at a depth of 2,311 meters and were collected from 2.7m above the sea floor. The chimney sample, GS18-ROV22-RO2, consisted of three chimney fragments, a, b, and c (**Figure 3**). GS18-ROV22-RO2c was crushed using a mortar and pestle into a slurry. The slurry was then divided into samples for enrichment cultures, measurements of sulfate reduction rates, and microbial community analysis. The top 2-5mm of

GS18-ROV22-RO2a was scraped into a 50ml Falcon tube using a sterile scalpel and mashed into a slurry. This slurry was used for measuring sulfate reduction rates and for microbial community analysis.

Figure 3 segments a (left), b (middle), and c (right) of chimney sample, GS218-ROV22-RO2, taken from the black smoker hydrothermal chimney, Camel, at LCVF.

2.2 Sulfate Reductions Rates

2.2.1 Preparation

In preparation, the solution was diluted to 37 MBq in a 20 ml Anti-Static vial using sterile, anoxic water. A 25% Zinc acetate solution was also made prior to sample collection and anaerobic synthetic seawater was made following methods used by Laso-Pérez et al. (2018). The synthetic seawater had a sulfate concentration of 28 mM, the sulfate concentration of seawater. An anoxic, substrate-free *Archaeoglobus* media, composed of Na_2SO_4, KCl, $MgSO_4 \cdot 7H_2O$,

$MgCl_2 \cdot 6H_2O$, NH_4Cl, $CaCl_2 \cdot 2H_2O$, $K_2HPO_43H_2O$, KH_2PO_4, NaCl, 0.2% Resazurin, Titriplex I, $MnSO_4 \cdot 2H_2O$, $CoCl_2 \cdot 6H_2O$, $ZnSO_4 \cdot 7H_2O$, $CuSO_4 \cdot 5H_2O$, H_3BO_3, $Na_2MoO_4 \cdot 2H_2O$, $NiSO_4 \cdot 6H_2O$, 0.2% $(NH_4)_2Fe(SO_4)_2 \cdot 6H_2O$, yeast extract, Na_2S, and dithionite, was also used.

2.2.2 $^{35}SO_4^{2-}$ Incubations

Samples were taken from GS18-ROV22-RO2 promptly after collection. The chimney rock samples were crushed with a steel mortar to make a rock slurry. Note that during the crushing and slurry formation, an anoxic environment was not maintained. To make the slurries, substrate-free *Archaeoglobus* media or synthetic anoxic seawater was added for homogenization and moisture. After crushing the chimney samples into a slurry, 2.5 ml of samples were transferred into exetainers. Four samples were made from mixing 2 ml GS-18ROV22-RO2c with 0.5 ml of the substrate-free *Archaeoglobus* media, four samples were made from mixing 2 ml GS-18ROV22-RO2c with 0.5 ml of the synthetic seawater, and four samples were made from mixing 2 ml GS-18ROV22-RO2a with 0.3 ml of the synthetic seawater. Less artificial seawater was added to these samples due to the more fluid consistency of the sample. Two blanks were made for each of the three slurry types, a sediment blank and a distillation blank. The exetainers were injected with a radioactive sulfur isotope, $^{35}SO_4^{2-}$, to measure reduction rate. Ten µl of the 50% $^{35}SO_4^{2-}$ solution was added to each sample and distillation blanks using a 10µl Hamilton syringe. The sediment blank was not injected with tracer and instead was immediately mixed with 5 ml of the zinc acetate solution and stored in a 50 ml Falcon tube at -20 °C. Promptly after the addition of the tracer, the distillation blanks were mixed with 5 ml of the zinc acetate solution and stored in a 50 ml Falcon tube at -20 °C. The remaining samples with the tracers, were incubated at 80 °C for 5 days. After incubation, all samples were mixed with 5 ml of the zinc acetate solution, vortex, and stored at -20 °C. Samples remained frozen until cold chromium reductions and scintillation counts were performed in the lab.

2.2.3 Cold Chromium Reduction of $H_2{}^{35}S$

The method used to reduce hydrogen sulfide with chromium used was based on the work of Fossing and Jørgensen (1989). The methods developed by Kallmeyer et al. (2004) used the work of Fossing and Jørgensen (1989) as a foundation and further adapted and optimized the process of using chromium to reduce hydrogen sulfide to obtain sulfate reduction rates. These methods developed by Kallmeyer et al. (2004) were used to obtain the sulfate reduction rates of the samples collected in this study. The following reagents were prepared in preparation for cold chromium reduction: 2 N HCl, 6 N HCl, 5% zinc acetate solution, 0.1 M citric acid, 0.5 M Na_2S, and 1 M $CrCl_3$ in 2 N HCl. A reduced $CrCl_2$ solution was prepared using the $CrCr_3$ solution. First, zinc pellets were submerged in 2 N HCl in a glass flask that was purged with N_2 gas for 20 minutes. The HCl was then drained and the $CrCl_3$ solution was added under continuous N_2 purging. Once the color change occurred from dark green to clear blue, indicating the reduction of $CrCl_3$ into a reduced $CrCl_2$ solution, the reduced $CrCl_2$ was then stored in syringes for use. The $CrCl_2$ solution was kept for up to one week before needed to be reduced again. Zinc pellets were rinsed after each use in 2 N HCl, by bubbling in 2 N HCl for 10 minutes. The flask was then emptied and zinc pellets were stored dry.

A distillation apparatus modelled after that used by Kallmeyer et al. (2004) was assembled (**Figure 4**). All glassware was connected and attached to the N_2 gas input. Five milliliters of the citric acid solution were added to each glass aerosol trap and mounted to the U-shaped glass tube. Using rubber tubing, a Pasteur pipette was then connected to the aerosol traps. Plastic tubes were used as zinc acetate traps, containing 5 ml of 5% zinc acetate solution and 1 drop of antifoam. These were connected so the Pasteur pipette was submerged halfway into the zinc acetate solution. Magnetic stir bars and 2 drops of antifoam were added to each reaction flask.

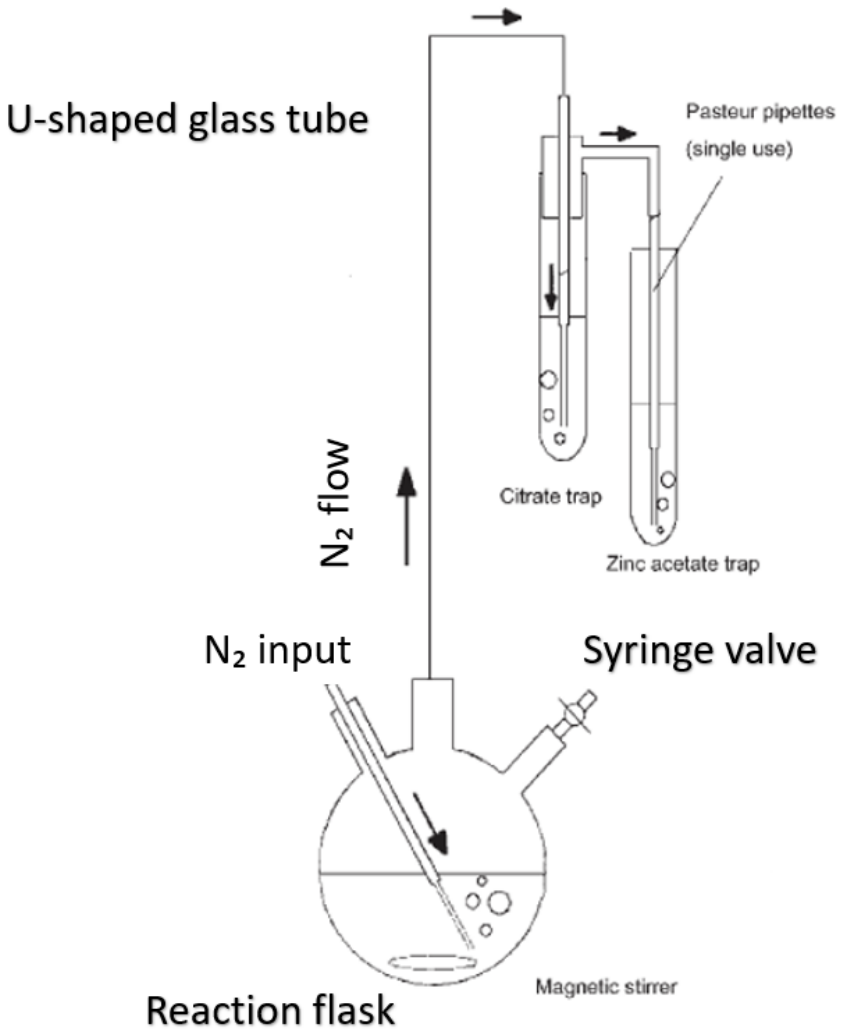

Figure 4 Diagram adapted from Kallmeyer et al. (2004) of the Cold chromium distillation apparatus used to measure SRR

Samples were all thawed for 20 minutes at room temperature and then centrifuged at 2,500 rotations per minute (RPM) for 5 minutes. Counting vials were prepared with 5 ml of 5% zinc acetate solution, including one vial to be used as the counter blank. After centrifugation, 100 µl of the supernatant was added to a counting vial with zinc acetate and the remaining supernatant was decanted into waste. Ten milliliters of dimethyl sulfoxide (DMSO) were added to each sediment vial, vortexed, and poured into a reaction flask. This was repeated for a total addition of 20 ml DMSO to the sediments in the reaction flasks.

Reaction flasks were then connected to a U-shaped glass tube in the distillation apparatus, the N_2 input, and attached with a syringe valve (**Figure 4)**. The gas was then turned on and adjusted until each zinc acetate trap had nitrogen flowing at a rate of 5 bubbles per second and flushed with gas for 10 minutes. To each reaction flask, 8 ml of 6 N HCl was then added through the syringe valve and the magnetic stirrers were set to 750 RPM. Next, 16 ml $CrCl_2$ solution was added to each reaction flask through the syringe valve. The gas was then adjusted as needed to return to a rate of 5 bubbles per second. The distillation then ran for two hours.

After two hours, the gas was shut off and the zinc acetate trap contents were poured into counting vials. The traps were flushed three times with 5 ml of scintillation fluid and the contents were poured into the counting vials. The counting vials containing the 100 µl of supernatant also had 15 ml of scintillation fluid added to each vial. All the vials were then carefully shaken holding the lid and run on the scintillation counter.

2.2.4 Porosity

The wet weight of each sample type was measured and then dried at 105 °C for three days. The dry weight was then measured and the porosity for each sample type was calculated by subtracting the dry weight from the wet weight.

2.2.5 Scintillation Counts and Reduction Rates

To count radioactivity, the PerkinElmer TriCarb® Liquid Scintillation Counter (PerkinElmer, USA) was used and the count conditions for one vial per sample was set to a count time of 20 minutes with 2 assay count cycles and 2 repeat sample counts. The counts per minute (CPM) were used for calculating rates. The CPM for the counter blanks, sediment blanks, and distillation blanks were averaged to obtain a value for the sample background (B_s). A detection limit was determined using the following formula (**Equation 2**):

Equation 2 the formula to determine the detection limit for measuring the sulfate reduction rates of a sample where B_s is equal to the sample background

$$detection\ limit = B_s + 3(standard\ deviation\ of\ blanks)$$

For each sample measurements, the sample background and detection limit were calculated using the counter blank from the same distillation group since only six distillations could be done each day including the sediment and distillation blanks from the sample slurry. For example, the detection limit for the samples from GS-18ROV22-RO2a distilled on November 16, 2018 was calculated using the counter blank from November 16th, 2018 and the sediment and distillation blanks taken from GS-18ROV22-RO2a. If the average CPM between the two counts for the samples was higher than the detection limit, the sulfate reduction rates could be calculated using the formula from Kallmeyer et al. (2004) (**Equation 3**).

Equation 3 The formula used by Kallmeyer et al. (2004) for calculating sulfate reduction rates of a sample where a_{TRIS} is the total reduced inorganic sulfur and a_{TOT} is the radioactivity found using the scintillation reads for CPM of the supernatant of the samples. P is the porosity and *t* is the incubation time in days.

$$SRR = [SO_4] \times P \times \frac{a_{TRIS}}{a_{TOT}} \times \frac{1}{t} \times 1.06 \times 1000$$

2.2.6 Radiation Safety and Management

During all sulfate reduction rate methods, radioactive safety measures were taken by creating designated areas for radio activity, using designated lab coats and safety goggles, and wearing two pairs of gloves. All radioactive waste was properly placed into radioactive waste bins and glassware was washed in 10% HCl acid between each use.

2.2.7 Microbial Community Analysis

To compare the sulfate reduction rates to the microbial community, the remainder of the slurries made from GS18-ROV22-ROC2 were stored at -20 °C and taken back to the Geomicrobiology lab in Bergen, Norway for analysis.

In order to collect a representation of the community, DNA extractions from both rock slurries were performed. Initially, 3 samples of 500 mg from the GS18-ROV22-ROCa slurry were taken, and 4 from GS18-ROV22-ROCc. The DNA was extracted using the MP Biomedicals™

FastDNA™ SPIN Kit for Soil (MP Biomedicals, LLC, Santa Ana, CA, USA). For higher DNA yields from extraction, five more replicates were taken from each slurry sample and additional steps were taken during the extraction protocol including: centrifugation for an extra 5 minutes after homogenization and incubating in a 55 °C water bath for 5 minutes after the addition of the binding matrix. DNA concentrations were measured using the Quantus™ Fluorometer (Promega Corporation, USA) to record the yield from the extractions.

To obtain sequences from the environmental sample, Ion Torrent 16S Amplicon Sequencing was carried out by Dr. Anita-Elin Fedøy in the Geomicrobiology lab at the K.G. Jepsen Center for Deep Sea Research (University of Bergen, Bergen, Norway) using the protocol as described in Hestetun et al. (2016). Sequences were obtained from amplicons using the Ion Torrent Personal Genome Machine platform technology (Life Technologies, USA).

Sequences obtained from the DNA extractions were then analyzed by Dr. Håkon Dahle at the K. G. Jepsen Center for Deep Sea Research (University of Bergen, Bergen, Norway).F Sequences were first filtered by removing sequences under 200 base pairs in size and sequences considered low quality with more than 2 expected errors. The sequences were then clustered into Operational Taxonomy Units (OTUs) for community analysis.

2.4 Cloning

Using the Gibson Assembly® method, developed by Gibson et al. (2009), genes encoding for the LDH subunits AF0806-AF0812 were inserted into the pET-21a vector. Gibson Assembly® is a method of joining DNA sequences without the use of restriction enzymes and is beneficial because it requires only a single isothermal reaction to assemble amplified vectors and inserts *in vitro* (Gibson et al., 2009). Gibson Assembly is also beneficial because the lack of restriction sites involved, which can be unfavorable because they may cause complications when located internally in the genes, where they may also introduce a “scar” by adding nucleotides that can lead to non-native amino acid residue becoming incorporating into expressed proteins (Celie et al., 2016).

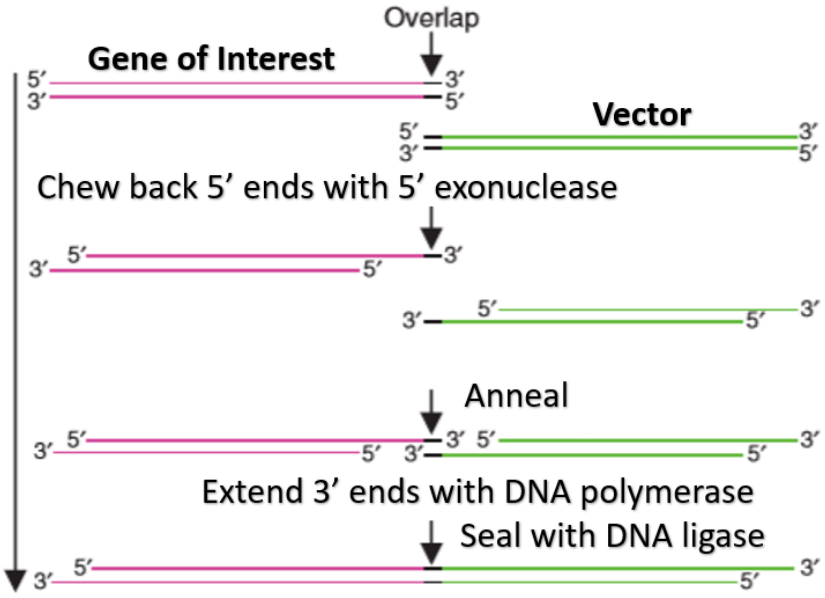

Figure 5 conceptualization of Gibson Assembly®. Adapted from (Gibson et al. (2009).

Information about the target genes was collected using available databases. The pI and molecular weight tool in the SIB ExPASy Bioinformatic Resource Portal (SIB Swiss Institue of Bioinformatics, Switzerland) was used to calculate pI for each protein. Previously published information on the size and mass of the proteins was also collected from UniProt (The UniProt Consortium, 2019).

2.4.1 Primer Design and Storage

In order to clone gene inserts target proteins into the pET-21a(+) vectors, forward and reverse primers for PCR-amplification of both the inserts and the vector were designed and obtained synthetically from Biomers (Ulm, Germany). The primers were designed to have unique overlapping DNA sequences for *in frame* cloning (**Table 1)**. When designing these primers, matching sequence overlap at annealing points were constructed to attach to the vectors and inserts in order for the complementary overhangs to be able to anneal to each other when the T5

exonuclease chews back at the 5' end of each portion (**Figure 5**). The primers are also designed to contain a stop codon to signal the stop of translation.

The pET-21a(+) vector contains a N-terminal T7 Tag® sequence and a C-terminus His-tag sequence. The T7 tag is an epitope tag that can be useful for its high-affinity antibodies and also in protein analysis and visualization. In order to allow for simpler protein purification after expression, a C-terminal His-tag was implemented on the amplified sequences. This feature allows for purification using immobilized metal affinity chromatography (IMAC), separating proteins in a mixture using specific binding properties. The primers were diluted and the concentrations were checked and corrected accordingly (Appendix B).

Table 1 Primers designed for Gibson Cloning of the LDH subunits from *A. fulgidus*.

Locus tag	NCBI annotation	Forward primer	Reverse primer	forward vector primer	reverse vector primer
AF0806	L-lactate permease	atggatgcaataagttgcagc	CTTTGTTAGCAGCCGGATCTCAGTGGTGGTGGTGGTGGTGaatcatttgtattttcaggatgaag	TTcaccaccaccaccaccactg	GCACCAATAGTATCGGTGTTGCTGCAACTATTGCATCCATatgtatatctccttcttaaagtt
AF0807	L-lactate dehydrogenase	atggagcgttacaacaagag	CTTTGTTAGCAGCCGGATCTCAGTGGTGGTGGTGGTGGTGaagcacaacagcttctttac	TTcaccaccaccaccaccactg	GGGGAACGTCAGCACCGACCCTCTTGTTGTAACGCTCCATatgtatatctccttcttaaagtt
AF0808	glycolate oxidase subunit	atgaagataacaaaagagcttgag	CTTTGTTAGCAGCCGGATCTCAGTGGTGGTGGTGGTGGTGtaccaccttccaggattga	TAcaccaccaccaccaccactg	CCTTACCAAGGATTTTCTCAAGCTCTTTTGTTATCTTCATatgtatatctccttcttaaagtt
AF0809	heterodisulfide reductase, subunit D	atgatcaagcctgagtatgt	CTTTGTTAGCAGCCGGATCTCAGTGGTGGTGGTGGTGGTGtcccaccaccatcgagaagt	caccaccaccaccaccactg	TTTCCGAAAGTAACTTAACTACATACTCAGGCTTGATCATatgtatatctccttcttaaagtt
AF0810	predicted coding region	atgaagattgtagaagctctgaag	CTTTGTTAGCAGCCGGATCTCAGTGGTGGTGGTGGTGGTGctttctcaccaccagcacta	AGcaccaccaccaccaccactg	CCTCCACTCCGTTCGCCTTCAGAGCTTCTACAATCTTCATatgtatatctccttcttaaagtt
AF0811	conserved hypothetical protein	atgaacatctacgatgctttgc	CTTTGTTAGCAGCCGGATCTCAGTGGTGGTGGTGGTGGTGgtcgagctttaatgcgagct	ACcaccaccaccaccaccactg	CCTTTATGGATTTTCTCCGCAAAGCATCGTAGATGTTCATatgtatatctccttcttaaagtt
AF0812	predicted coding region	atgcttggcaagcttctcca	CTTTGTTAGCAGCCGGATCTCAGTGGTGGTGGTGGTGGTGgaggcaccagcttctcgcca	TCcaccaccaccaccaccactg	AATAAGCTTTGAGGACTTTCTGGAGAAGCTTGCCAAGCATatgtatatctccttcttaaagtt

2.4.2. Amplification of Gene Inserts and Vector

For the genes of interest and the vector, the PCR reaction protocols described in **Table 2** and **Table 3** were followed. Prepared reaction mixes were kept on ice until the thermocycler reached the initial denaturation temperatures. Annealing temperatures were calculated by the following equation (**Equation 4**) and by checking annealing temperature using the ThermoFischer Scientific T_m Calculator (Thermo Scientific™ T_m Calculator, Waltham, MA, USA).

Equation 4 The formula used to determine annealing temperatures of inserts and vectors for PCR using the melting temperatures estimated from the sequences.

$$T_a = T_m(lower\ reaction) + 1\ °C$$

For AF810, the PCR was repeated at an annealing temperature of 65 °C.

Table 2 PCR protocol for the reaction mix for amplification of genes of interest (AF0806-AF0808 and AF0810-AF0812) and pET-21a(+) vector

Genes of Interest	**Vector**	**Volume (µl)**
10 µM forward primer	10 µM forward primer	1.25
10 µM reverse primer	10 µM reverse primer	1.25
NEB Q5 high-fidelity 2X Master Mix	NEB Q5 high-fidelity 2X Master Mix	12.5
Archaeoglobus DNA (1ng-1µg)	pET-21a(+) 1:10 dilution 50ng/µl	1.0
Nuclease free H_2O	Nuclease free H_2O	9.0
	Total:	**25.0**

Table 3 Protocol for the thermocycling of the PCR of amplification of genes of interest (AF0806-AF0808 and AF0810-AF0812) and pET-21a(+) vector

Genes of Interest		
Stage	**Temperature (°C)**	**Time**
Initial Denaturation	98	10 minutes
30 Cycles	98	10 seconds
	48	30 seconds
	72	2.5 minutes
Final Extension	72	2 minutes
Hold	4	∞

Vector		
Stage	**Temperature (°C)**	**Time**
Initial Denaturation	98	30 seconds
30 Cycles	98	10 seconds
	63	30 seconds
	72	2.5 minutes
Final Extension	72	2 minutes
Hold	4	∞

2.4.3 Gibson Assembly of Vectors and Inserts

To create the expression vectors for each gene of interest, amplified genes of interests and vectors were assembled into the pET-21a(+) vectors following the Gibson Assembly® Protocol (E5510) (New England BioLabs, Ipswich, MA, USA) (**Table 4**). The success of the assembly reactions were verified by gel electrophoresis on a 1% agarose gel.

The PCR product was digested with *Dpn*1 restriction endonuclease in order to destroy the plasmid template before setting up the Gibson Assembly reaction. This was performed by mixing 5 µl of the PCR product with 1 µl CutSmart® Restriction Enzyme Buffer, 1 µl *Dpn*I, and 3 µl Milli-Q H_2O for a reaction total of 10 µl. The reaction incubated for 30 minutes at 37 °C and then was heat shocked for 15 minutes at 80 °C. The Gibson Assembly of the inserts into vectors

was then performed using reaction mixture was made according to **Table 4** to form expression vectors**.** The reaction was heated at 50 °C for 40 minutes. The time of the heat incubation was based on the estimated concentrations of the inserts and vectors determined from the gel electrophoresis.

Table 4 Protocol for the Gibson Assembly Reaction mix where 3x is recommended to be between 0.02 and 0.5 pmols of DNA (New England BioLabs, Ipswich, MA, USA).

	Volume (µl)
Gibson Assembly Master Mix (2X)	10.0
UV treated Milli-Q H_20	(10.0-3x)
Insert	2x
pET-21a(+) vector	x
Total:	**20.0**

2.4.4 Gel Electrophoresis

All DNA gel electrophoresis tests in this study were run on 1% agarose gels. In order to make the 1% agarose gels, a solution of 40 ml 1X TAE Buffer was mixed with 0.4 g agarose and heated in a microwave until agarose was dissolved, but not to the point of boiling. Once cooled, 4 µl of 100X concentrated GelGreen™ nucleic acid dye (Biotium, Inc., Fremont, CA, USA) was added and the solution was poured into the mold and covered until it was set. Samples were by pipetted up and down into one drop of BBS gel loading dye, a bromophenol blue and sucrose 10X solution by MP Biomedicals™ (MP Biomedicals, LLC, Santa Ana, CA, USA), . The mix was then loaded into wells. For the DNA standards, 5 µl of either the GeneRuler™ 100 bp Plus DNA Ladder or Lambda DNA/EcoRI+HindIII Marker by Thermo Scientific™ were used (Thermo Scientific™ , Waltham, MA, USA). The gel electrophoresis was run on 50 volts for 30 minutes on the PowerPac™ Basic Power Supply (Bio-Rad Laboratories, Hercules, CA, USA). Gels were imaged using Syngene G:Box UV Transilluminator (Syngene, Cambridge, UK).

2.4.5 Transformation of Expression Vectors

The assembled plasmids from the Gibson Assembly reaction were then transformed into NEB 5-alpha Competent *E. coli* (NEB #C2987) cells using the NEB Gibson Assembly Cloning Kit (New England BioLabs, Ipswich, MA, USA). Following the kit protocol, 2 µl of the assembled plasmids were added to the given aliquot of cells. The cells were given a slight shake and then incubated on ice, undisturbed for 30 minutes. After the incubation, cells were heat shocked at 42 °C for 30 seconds and then cooled on ice for 2 minutes. Next, 950 µl of SOC medium was added and the cells were incubated in a rotating incubator at 37 °C and 250 RPM. After shaking for 60 minutes, the cells were plated on LB agar plates containing 100 µg/ml of ampicillin and incubated overnight at 37 °C.

2.4.6 Colony PCR

In order to quality check for the success of the Gibson Assembly reaction, colonies were picked from the plated cells for a PCR. The PCR protocols found in **Table 5** and **Table 6** were used and the products of the colony PCR were run on a 1% agarose gel using gel electrophoresis.

Table 5 Protocol for the colony PCR reaction mix

	Volume (µl)
pET-21a(+) forward primer	1.25
pET-21a(+) reverse primer	1.25
Q5 Master Mix	12.5
UV Milli-Q H_20	9.0
Total:	**24.0**

Table 6 Protocol for the thermocycling for colony PCR

Stage	Temperature (°C)	Time
Initial Denaturation	95	5 minutes
30 Cycles	94	30 seconds
	48	30 seconds
	72	2.5 minutes
Final Extension	72	2.5 minutes
Hold	4	∞

2.4.7 Plasmid Purification

Pre-cultures were inoculated from the LB agar plates in liquid LB medium containing 100 µg/ml of ampicillin because of the ampicillin resistance in the competent cells used, which aids in selection and protection against contamination.

The plasmids were then purified using Monarch® Plasmid Miniprep Kit and protocol (New England BioLabs, Ipswich, MA, USA). To purify the plasmids using the Monarch® Plasmid DNA Miniprep Kit, the Plasmid Wash Buffer 2 first needed to be prepared by adding ethanol in a 4:1 ethanol to buffer ratio. All centrifugations in the purification procedure were carried out at 13,000 RPM.

To ensure the success of the Gibson Assembly and to quality check for accurate assemblage of the inserts into the vectors, Sanger sequencing was performed on the purified plasmids at the

Sequencing Facility (University of Bergen, Bergen, Norway). The automated Sanger DNA Sequencing was run with the Applied Biosystems 3730XL Analyzer (Applied Biosystems, Foster City, CA, USA), which is a high-throughput, capillary-based system and analyzes DNA fragments that have been fluorescently labelled with Big Dye version 3.1. The protocols in **Table 7** and **Table 8** were used for the reaction mix and thermocycling, respectively.

Table 7 Protocol for the Sanger sequencing reaction mix

	Volume (µl)
Big Dye v3.1	1.0
Sequencing Buffer	1.0
Plasmid	X(200-250ng)
Primer	1.0
UV Milli-Q H_20	7-X
Total:	**10.0**

Table 8 Protocol for the thermocycling of the PCR for Sanger sequencing

Stage	**Temperature (°C)**	**Time**
Initial Denaturation	96	5 minutes
25 Cycles	96	10 seconds
	53	5 seconds
	60	4 minutes
Hold	4	∞

2.4.8 Transformation of Plasmids into Expression Vector

Purified plasmids containing the target inserts were then transformed into the BL21-Codon Plus (DE3)-RIL competent *E. Coli* cells (Agilent, Santa Clara, CA, USA). The BL21-Codon Plus (DE3)-RIL competent *E. Coli* cells allow for high expression of heterologous (non-native) proteins. High levels expression can be achieved because the extra tRNAs in BL21-CodonPlus cells help to optimize translation of the proteins and consequently, expression. The BL21-CodonPlus (DE3)-RIL cells also allow for the incorporation of rare (RIL) codons, that prevent

the restriction of translation from codon bias that can impede expression (Carstens et al., 2001). Since the pET-21a(+) vector has the T7 RNA polymerase promoter, a BL21-CodonPlus (DE3) strain was chosen due to the design of the strain being optimal for expressions that use the T7 RNA polymerase promoter to offer high-level transcription of clones (Studier and Moffatt, 1986).

First, a procedure based on Pope and Kent (1996) was used for rapid transformation. This method is hereby referred to as "Righteous" transformation, offers a quicker and simpler transformation of purified DNA fragments in comparison to the heat-shock method that was called for in the protocol for the BL21-Codon Plus (DE3)-RIL competent cells. For the "Righteous Transformation," the cells were thawed on ice from being stored at -80 °C. LB agar plates containing 100 μg/ml ampicillin and 50 μg/ml chloramphenicol were warmed to 37 °C during the thawing. A 1:10 dilution of β-mercaptoethanol in dH_2O was prepared and 2 μl of the solution was added to each 100 μl aliquot of competent cells. For each transformation reaction, 15 μl of cells were aliquoted. To the aliquots, 20-50 ng of DNA were added and gently mixed by pipetting. One aliquot was used as a positive control and had 2 μl of Puc18 control plasmids added to it. The aliquots were then incubated on ice for 90 minutes and plated on the warm LB agar plates. The plates were incubated overnight at 37 °C.

To increase the success of the transformation of AF0809, transformations were repeated using the heat-shock transformation protocol given with the BL21-Codon Plus (DE3)-RIL competent cells.

In order to check for the success of the transformations, another colony PCR was carried out, using the same procedure as described in the section above. Three colonies were picked from the LB agar plates and a colony PCR was performed to verify the clone to be used expression and indicate the likelihood of colonies containing the expression vectors after transformations.

2.4.9 Protein Expression

Colonies confirmed by colony PCR were used to inoculate LB broth cultures. To begin, pre-cultures were started by colonies were picked from LB agar plates. Using a pipette tip, a single

colony from each plate was selected and inoculated into LB broth with 100 μg/ml of ampicillin and 50 μg/ml of chloramphenicol. For AF0806, AF0807, AF0808, AF0811, and AF0812, precultures of 2.5 ml were made and incubated over night at 37 °C, shaking at 225 RPM overnight. The next day, pre-cultures were then added to 100 ml of LB broth with the same concentrations of antibiotics as the pre-culture and incubated at 37 °C, shaking at 225 RPM. Growth rates were measured using a spectrometer and following the optical density (OD) at 600 nm. Once the OD_{600} was between 0.4 - 0.6, glycerol stocks were made and induction using isopropyl β-D-1 thiogalactopyranoside (IPTG) was initiated. Glycerol stocks were made for each clone using 340 μl of 70% glycerol and mixing it with 640 μl of the culture and then stored at -80 °C in order to obtain a bank of 25% glycerol stocks for each clone to work from for future culturing. To induce protein expression, IPTG was added to the expression culture to a concentration of 1 mM. IPTG is a reagent that triggers transcription of the lac operon by mimicking allolactose and due to the lac operon controlling the production of some proteins, targeted proteins can be produced after it is triggered (Neubauer et al., 1992). The design of the pET-21a(+) vector has a location of the lac operon to induce the production of proteins coded by the genes of interest.

Once induced with IPTG, the cultures were allowed to grow in the same conditions for two hours. Before and after the induction, two 500 μl aliquots from cultures were taken and centrifuged at 13,000 RPM for 10 minutes and stored for sodium dodecyl sulfate-polyacrylamide gel electrophoresis (SDS-PAGE) gel analysis of protein production. When the cultures reached OD_{600} of 1.10, they were distributed into 50 ml Falcon tubes and centrifuged at 3,000 RPM for 15 minutes. The supernatant was discarded and the cell pellet was stored at -20 °C.

Multiple attempts were carried out for AF0806 and AF0807 cultures before an OD_{600} of around 1.10 was reached. To do this, pre-cultures were made from colonies formed on plates streaked out from glycerol stocks. In the second trials, cultures were initially grown in the same incubation conditions as the first, but with concentrations of 0.75 mM IPTG. After induction, the temperature was lowered to 27 °C and cultures were incubated for 6 hours. In the third trials, the concentration of IPTG used was again 1 mM, but the cultures were incubated at 20 °C during the entire incubations to provide conditions for slower growth.

For efforts to produce soluble proteins of AF0809, incubations were repeated at 175 RPM at 20 °C. A 100 ml culture of AF0809 was induced with 0.5 mM IPTG, a 200 ml culture with 1 mM IPTG, and another 100 ml culture with 2 mM IPTG. All three cultures of AF0809 were then incubated overnight until the OD_{600} was over 1.0. The cultures were then transferred to 50 ml Falcon tubes and centrifuged at 3,000 RPM for 15 minutes, the supernatant was discarded, and the pellet was then frozen and stored at -20 °C. Two aliquots of 500 µl were taken from each culture batch, both before and after induction, for SDS-PAGE gel analysis.

2.4.10 Solubility of Proteins

To isolate proteins, 5 grams of the frozen induced pellet from the 1 L cultures were then lysed in 5 ml phosphate lysis buffer, composed of phosphate buffer A and a 0.25 mg/ml of lysozyme. The cells were gently mixed and then incubated on ice for 30 minutes. After incubations, samples were sonicated at an amplitude of 27% in 5 intervals of 8 to 10 seconds. Between intervals, samples were cooled on ice for 10 seconds. Subsamples of 16 µl of the crude lysate were taken for later SDS-PAGE analysis. Lysed samples were centrifuged at 13,000 RPM for 3 minutes and 30 seconds. The supernatant, or clear lysate, was transferred to fresh centrifuge tubes. Subsamples of 16 µl of supernatant were also taken for later SDS-PAGE gel analysis to show the contents of the clear lysate.

2.4.11 Purification of Proteins

To purify the proteins using Immobilized metal affinity chromatography (IMAC), the Bio-Rad BioLogic LP chromatography system (Bio-Rad Laboratories, Hercules, CA, USA) was first used. The BioLogic LP chromatography system was cleaned before each use by flowing Milli-Q water at a rate of 2.0 ml per minute for about 5 ml through both input tubes. Then the rate was dropped to 0.5 ml per minute to add the Bio-Rad Profinity™ IMAC Resin column (Bio-Rad Laboratories, Hercules, CA, USA) and brought back up to the original rate.

Immobilized metal affinity chromatography (IMAC) was used to purify the proteins based on the strong affinity histidine-tagged (His-tagged) molecules have for metal ions. To start, the system was first flushed with Buffer A, by putting both input tubes in Buffer A, for 5 minutes. Clear

lysate was then filtered through 0.2 µl filters and loaded into a 5 ml syringe. The syringe with the 2.0 ml of sample was then placed onto the BioLogic LP chromatography system and loaded into the sample tube. The switch was rotated so the sample would be run through the system and the column. The two input tubes were then placed into the appropriate buffers and the program was set on the BioLogic LP chromatography system. When the samples finished running through the column, the purified proteins were then eluted by the gradual addition of Elution Buffer B and collected in fractions, contents of the fraction tubes could be identified using the chromatograms. The BioLogic LP chromatography system was rinsed with Milli-Q water after each sample and then filled with 20% ethanol and shut off after each day of use. The columns were flushed with 20% ethanol and removed to be stored at 4 °C.

The proteins that were soluble and successfully purified using the IMAC columns were then produced in larger quantities. One-liter cultures were grown following the same protocol as the 100 ml cultures for each clone. The fractions containing the proteins from the soluble samples were identified from the SDS-PAGE gel analysis.

2.4.12 Concentration of Fractions

Some fractions containing the purified proteins were combined and concentrated in order to obtain a higher concentration of proteins per sample. This was done by taking one 4.0 ml fraction and centrifuging it in an Amicon® Ultra Centrifugal Filters with Ultracel® generated cellulose filters with a cut-off of 30 kDa (Merck Millipore, Burlington, MA, USA). The protein solution was centrifuged for 2 minutes at 4,000 RPM and then an additional fraction was added to the tube and this step was repeated until there was 500 µl of sample in the tube. The sample was first pipetted up and down against the filter to loosen any proteins that might be stuck to the filter and then transferred into a 2.0 ml Eppendorf microcentrifuge tube.

2.4.13 SDS-PAGE Gel Analysis

The SDS-PAGE gels used in this study were GenScript ExpressPlus™ PAGE Gels, size 10 by 8, with a concentration gradient of 8 to 16% and a separation range of 160 to 10 kDa (GenScript Biotech Corporation, Nanjing, China). The gels contain 12 well with a loading volume maximum of 60 µl (ibid.). The SDS-PAGE gel electrophoresis was run on Tris-MOPS-SDS Running Buffer (MOPS running buffer) made from 1 liter distilled water and one MOPS running buffer Powder packet from GenScript (ibid.). The samples of uninduced culture (UI), induced culture(I), crude lysate, and clear lysate were all run through SDS-PAGE gel analysis, as well as samples from purified protein fractions and stored aliquots. For all the samples containing *E. coli* cell material (UI, I, and crude lysate), 20 µl of MOPS running buffer and 20 µl of 5X sample buffer by GenScript (GenScript Biotech Corp., Nanjing, China) were added and mixed to improve viscosity. For all other samples, the 5X sample buffer was added to each sample in a ratio of 1 µl of buffer to 5 µl of sample. All samples were mixed and incubated on a shaker at 300 RPM at a temperature of 95 °C for 10 minutes. Samples were then spun down and 20 µl were loaded into a SDS-PAGE gel. The gels were run for 50 minutes at 140 volts on the Bio-Rad PowerPac™ Basic Power Supply (Bio-Rad Laboratories, Hercules, CA, USA). The Bio-Rad Precision Plus Protein™ Dual Color Standard (Bio-Rad Laboratories, Hercules, CA, USA) was used as the protein standard in quantities of 5 µl for all gels.

2.4.14 Gel Filtration of Proteins

The purified proteins were then filtered on a 120 mL gel filtration column to separate the proteins by size on the AKTÄ START (GE Life Sciences, Marlborough, MA, USA). The flow rate was set to 1.0 ml per second and they were run with the HEPES running buffer in a room at 4 °C. The collected fractions of were run on an SDS-page gel to identify which fraction contained the proteins of interest. Once identified, the buffer of these fractions was exchanged to a storage buffer using Amicon® Ultra Centrifugal Filters. It was then stored in the HEPES storage buffer at -20 °C until further analysis. The concentrations of the frozen aliquots were measured using the Quantus™ Fluorometer (Promega Corporation, Fitchburg, WI, USA) to obtain a protein concentration estimate.

2.4.15 Circular Dichroism

For circular dichroism analysis (CD) on AF0808, the protein samples needed to be in a buffer without chloride ions because below 200 nm, chloride ions are strongly absorbent (Kelly et al., 2005). Therefore, a second buffer exchange was done for AF0808. This was first attempted to be done through dialysis using a D-Tube Dialyzer Maxi (EMD Millipore Corporation, Burlington, MA, USA) to change to a storage buffer with fluoride anions instead of chloride. However, a second buffer exchange procedure was necessary and executed using the gel filtration column on the AKTÄ system with the same protocol as the size exclusion. The fractions containing the protein were isolated by analyzing on SDS-Page gels and then combined and concentrated using the Amicon® Ultra Centrifugal Filters. The concentrations of the samples were measured on Quantus, Nanodrop, and Quick-Read, due to inconsistencies between the concentration readings on the different devices. Once a sample concentration of at least 0.05 milligram per milliliter was obtained, the CD spectra of the sample was run on the Jasco J-810 Spectropolarimeter. First the sample was run at 20 °C from 190 nm to 260 nm, and then the temperature scan was run to determine the melting point of the protein. This ran from 20 °C to 95 °C, and then for an additional 10 °C to get a clearer image of the melting curve. Once the sample appeared to be denatured, the spectropolarimeter was run again from 190 nm to 260 nm at 105 °C. This entire process was repeated with a blank sample of buffer in order to eliminate noise caused by the buffer on the reading of AF0808. Data was collected using the Spectra Manager software version 1.55.00 for Windows 95/NT by Jasco.

Using the molecular weight, protein concentrations, and number of amino acids in the protein, the percentage of alpha helices were estimated using the software program, CD Spectra Deconvolution version 2.1 (CDNN), which estimates secondary structure of a protein.

2.4.16 Concentration Measurements

a.) To measure the concentrations of DNA and proteins on the Quantus™ Fluorometer (Promega Corporation, USA). Two separate protocols were followed to estimate concentrations of DNA and for protein concentration estimates (Appendix A).

b.) To obtain protein concentration measurements of the Thermo Scientific™ NanoDrop 2000 Spectrophotometer (Thermo Scientific™, Waltham, MA, USA), 2.0 µl of sample was loaded on the pedestal. First the blank of the buffer without the proteins was read, and then a 2.0 µl sample containing the proteins. The software program that collected this data was The NanoDrop 2000/2000c software version 1.6.198 by Thermo Scientific™ (Thermo Scientific™, Waltham, MA, USA).

c.) The Direct Detect™ Spectrometer (EMD Millipore Corporation, Burlington, MA, USA) was the third method used to measure protein concentrations. This machine measures amide bonds using infrared light beam against a hydrophilic polytetrafluoroethylene membrane containing the dried sample on the Direct Detect™ Assay-free Card. The data collected from the Direct Detect™ was processed using the Direct Detect™ software version 3.0.21.0.

3.0 Results

3.1 Sulfate Reduction Rates

3.1.1 Measured Sulfate Reduction Rates

Sulfate reduction rates were detected in four of the twelve samples taken. Two samples from GS18-ROV22-ROCa mixed with synthetic seawater had sulfate reduction rates of 0.142 $\text{nmol g}^{-1}\text{ day}^{-1}$ and 0.422 $\text{nmol g}^{-1}\text{ day}^{-1}$. The other two samples were from GS18-ROV22-ROCc that were mixed with synthetic seawater and had rates of 0.201 $\text{nmol g}^{-1}\text{ day}^{-1}$ and 0.769 $\text{nmol g}^{-1}\text{ day}^{-1}$ (calculations and data can be count in Appendix C.1). The counts from the scintillation reader were below the detection limit for all samples from GS18-ROV22-ROCc

with *Archaeoglobus* media and for the remain samples mixed with seawater from both rock fragments..

3.1.2 Microbial Community Analysis

Of the four samples of DNA from GS18-ROV22-ROCc initially extracted, only one sample had a detectable DNA concentration, and zero of the three from GS18-ROV22-ROCa. The experiment was then repeated with additional steps taken to increase the yield of extraction. Five additional samples were taken from each rock. The two samples that had detectable DNA concentrations came from GS18-ROV22-ROCa, while the concentrations of DNA in the remaining eight samples read lower than the blank (**Table 9**).

Table 9 Concentrations of DNA extracted from GS18-ROV22-ROCa and GS18-ROV22-ROCc collected from LCVF. "LTB" indicates a concentration measurement that was than the blank when measured on Quantus™ Fluorometer (Promega Corporation, USA)

Sample	Rock	DNA concentration (ng/µl)
1	GS18-ROV22-ROCc	0.257
2	GS18-ROV22-ROCc	LTB
3	GS18-ROV22-ROCc	LTB
4	GS18-ROV22-ROCc	LTB
5	GS18-ROV22-ROCa	LTB
6	GS18-ROV22-ROCa	LTB
7	GS18-ROV22-ROCa	LTB
1a	GS18-ROV22-ROCa	LTB
2a	GS18-ROV22-ROCa	LTB
3a	GS18-ROV22-ROCa	0.114
4a	GS18-ROV22-ROCa	0.0098
5a	GS18-ROV22-ROCa	LTB
1c	GS18-ROV22-ROCc	LTB
2c	GS18-ROV22-ROCc	LTB
3c	GS18-ROV22-ROCc	LTB
4c	GS18-ROV22-ROCc	LTB
5c	GS18-ROV22-ROCc	LTB

Only the two samples from GS18-ROV22-ROC2a produced a high enough concentration of DNA after PCR amplification for sequence analysis. After filtration of sequences, 77.1% of sequences from sample 3a and 77% of sequences from 4a were used to be clustered into OTUs. Results were obtained from Dr. Dahle through personal communications and indicated that there were no *Archaeoglobus* present in the sample, but there was a presence of sulfate reducing bacteria. In sample 3a, *Thermodesulfobacteriaceae* were found with a relative abundance of less than 0.1% and in sample 4a, *Desulfohalobiaceae* had a relative abundance of 0.1%.

3.3 Cloning

The number of amino acids, the mass (Da), and the pI was researched and recorded for the components of the putative lactate dehydrogenase complex, lactate permease, and lactate dehydrogenase that were explored in this study (**Table 10**).

Table 10 Descriptions of genes from the putative lactate dehydrogenase complex

Locus tag	Locus	NCBI annotation	Number of Amino Acids	Mass (Da)	pI
AF0806	*lctP*	L-lactate permease	544	57084.04	9.04
AF0807	*lldD*	L-lactate dehydrogenase	366	41015.69	5.97
AF0808	*dld*	glycolate oxidase subunit	461	50391.23	5.91
AF0809	*lldE*	heterodisulfide reductase, subunit D	300	34250.77	8.53
AF0810	*lldG*	predicted coding region AF_0810	123	13572.73	6.98
AF0811	*lldF*	conserved hypothetical protein	364	41158.76	6.3
AF0812	-	predicted coding region AF_0812	298	34385.41	4.99

3.3.1 Gibson Assembly®

The vectors and the genes of interest were successfully amplified using PCR with the designed primers, except for the AF0810 gene inserts that had no apparent PCR products. **Figure 6** depicts these results on the 1% agarose gel from the gel electrophoresis of the PCR products from the

amplifications. The PCR for AF0810 was re-run at a higher annealing temperature that was more suitable and specifically calculated using the melting temperature of AF0810 (**Equation 4**), however there was still a lack of PCR product from this reaction. The amplified genes of interest and vectors were then assembled using the Gibson Assembly reaction protocol transformed into the NEB 5-alpha Competent *E. coli* cells.

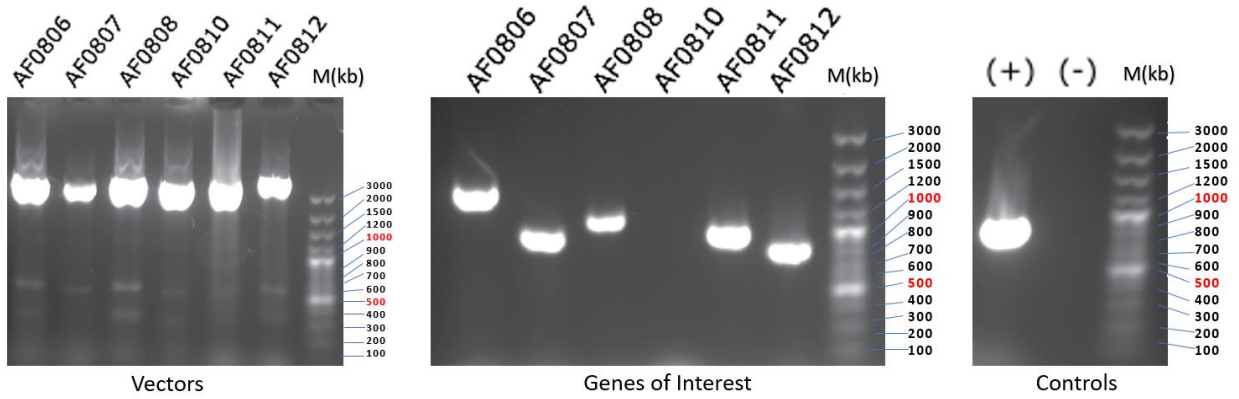

Figure 6 PCR products of the amplified putative LDH genes of interest from *A. fulgidus* and the pET-21a(+) vectors. Products were run on 1% agarose gel using gel electrophoresis. The positive control (+) was a successfully amplified AF0809 gene from *A. fulgidus* from a previous study in the lab. The negative control (-) was UV treated Milli-Q water. The DNA markers on the right of each gel are the GeneRuler™ 100 Plus bp DNA Ladder.

3.3.2 Transformation of Assembled Vectors

To confirm successful assembly of *A. fulgidus* gene inserts AF0806, AF0807, AF0808, AF08011, and AF0812 into the pET-21a (+) plasmids, colony PCR was performed using the NEB 5-alpha Competent *E. coli* cells containing assembled plasmids. To visualize the success of assembly, the colony PCR products were run on 1% agarose gel (**Figure 7**). The five candidates reflected the estimated sizes of the assembled genes of interest into the plasmids, in comparison to the DNA standard used. The pET-21a(+) plasmid containing the AF0809 gene had previously been assembled successfully in an earlier study. The plasmids were then purified and sequences obtained from Sanger sequencing confirmed that the vectors contained the desired genetic insert (not shown). The purified plasmids containing the genes of interest were then used for the remaining part of this study.

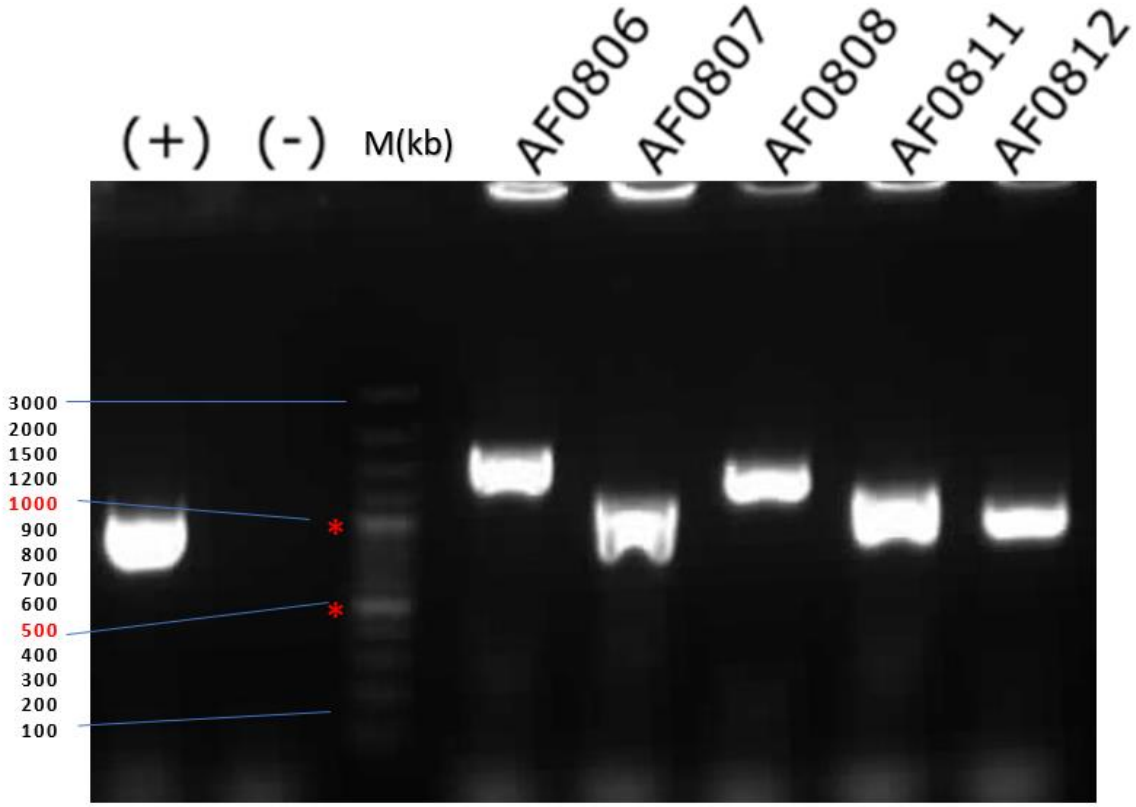

Figure 7 1% agarose gel electrophoresis image from the assembled vectors and *A. fulgidis* gene inserts. The positive control (+) was a successfully assembled *pET-21a(+)* vector with the AF0809 insert from a previous study and the negative control (-) was UV Milli-Q water. The DNA marker used was Thermo Scientific™ GeneRuler™ Ready-to-use 100bp Plus DNA Ladder

3.3.3 Transformations to Expression Vectors

To produce proteins from coded from the ORFs, the purified plasmids were transformed into BL21-Codon Plus (DE3)-RIL competent *E. coli* cells. After transformations, colony PCR was conducted from the plated colonies of competent cells. This was performed in order to verify the success of the transformation. The first transformations were executed using the righteous transformation method. The results from these transformations method were successful for most candidates; however, it was unsuccessful for AF0809 (**Figure 8a**). Conversely, the transformation of the AF0809 plasmid was then successful when repeated using the Heat Shock transformation protocol for the BL21-Codon Plus (DE3)-RIL competent cells (**Figure 8b**). The

colony PCR was performed in triplicates for each transformation in order to show the strength of success of the transformations and likelihood that plated colonies contained cells with the assembled plasmids (**Figure 8b,c**).

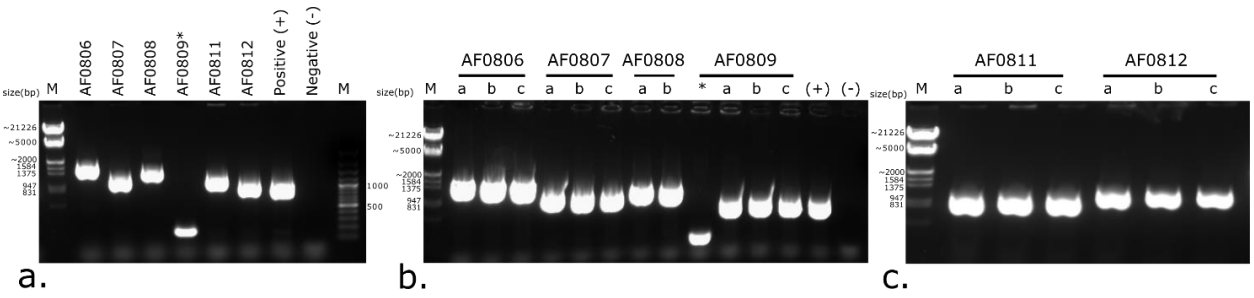

Figure 8 1% agarose gels of colony PCR of clones containing the genes for *A. fulgidus* LDH complex cloned pET-21a(+) into vectors and transformed into BL21-Codon Plus (DE3)-RIL competent *E. coli* cells. The DNA ladders on the left of each gel are λ*EcoRI/HindIII* ladders and on the right for gel "a." is a 100bp ladder. **a.** The gel for all clones from "Righteous" transformations; positive control was a confirmed successful transformation using BL21-Codon Plus (DE3)-RIL competent cell transformation protocol of AF0809 from a previous study **b.** Replicates from different colonies for AF0806, AF0807, AF0808 from the "Righteous" transformations. AF0809***** was the colony from the "Righteous transformations" and the replicates are from a second transformation attempt following the protocol for the BL21-Codon Plus (DE3)-RIL cells **c.** Replicates of colonies from the "Righteous" transformations of AF0811 and AF0812. The marker used was

3.3.4 Expression of Target Proteins

In the first incubations of the batch culture of AF0806 clones, absorbance decreased in the clones after induction with IPTG (data shown in Appendix C.2). In a second trial where cultures were grown overnight at 20 °C, instead of 37 °C, the cell density did not decrease, however it did increased more slowly than with other clones incubated in the same conditions (Appendix C.2). The first incubation of the batch culture of AF0807 clones showed a slowing of the rate of increased absorbance over time after the addition of IPTG, but when conditions were adjusted for slower growth, as with AF0806 cultures, this was not observed. **Figure 9** shows the SDS-PAGE gels of the cultures before and after induction with IPTG. Successful production of the target proteins occurred in the batch cultures of AF0808, AF0809, AF0811, and AF0812 clones, as observed by the darker bands in the induced (I) lanes in comparison to the lanes containing the uninduced (UI) sample.

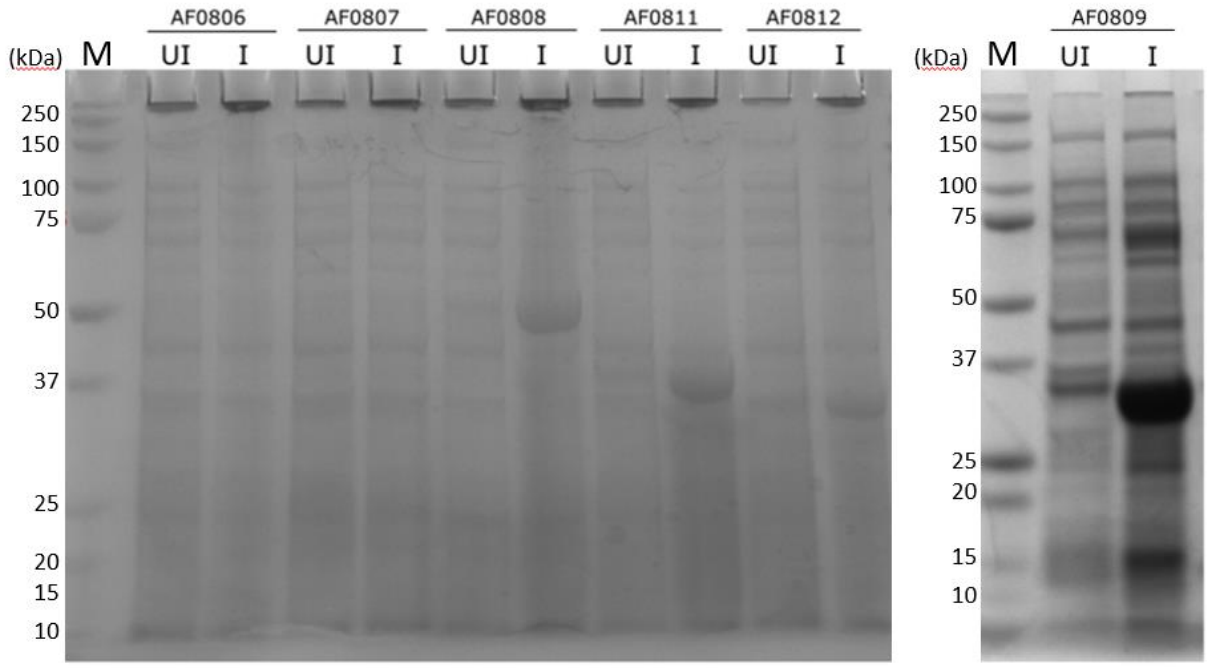

Figure 9 SDS-PAGE gel of clones containing genes for putative LDH from *A. fulgidus.* UI lanes show the composition of the cells prior to induction with IPTG. I lanes are from cultures grown to an OD_{600} over 1.0. The Protein Standard (M) used was the Bio-Rad Precision Plus Protein™ Dual Color Standard.

4.3.5 Purification of Expressed Proteins

After lysing cells and running on SDS-PAGE gels, soluble proteins were observed only from clones containing genes for AF0808, AF0811, and AF0812. Induction was repeated with slower growth conditions and varying concentrations of IPTG with AF0809 clones to obtain soluble proteins, however protein remained insoluble in all attempts. Nonetheless, purification of all four proteins produced was attempted. As seen in **Figure 10,** proteins were purified from AF0808, AF0812, and AF0811 clones. The chromatograms show initial large peaks from the sample loading and flow through. After elution with a gradient of Buffer B, a second peak is visible for proteins from AF0808 and AF0812 in fractions 8 and 9. The results from SDS-PAGE gel electrophoresis confirm the fractions contained purified proteins from AF0808 and AF0812, despite not having a clear second peak on the chromatogram. The bands on the gel from the concentrated fractions from AF0811 are indicative of purified proteins. However, it is important

to note the proteins produced and purified from AF0811 were not the expected size for the target protein, and were not the same size as the band displaying expression (lane 2). The purification also did not produce an entirely pure protein as observed by the multiple bands in the purified fraction lanes (lanes 8 and 9), and of which neither matched the expected size of near 41 kDa of the target protein. No proteins were able to be purified in AF0809, due to the insolubility of the proteins. This is confirmed by the lack of bands showing expression in the lanes with clear and filtered lysate, from the lack of visible bands in eluted fractions of the SDS-PAGE gel, and from the lack of a second peak in the chromatogram from the protein elution.

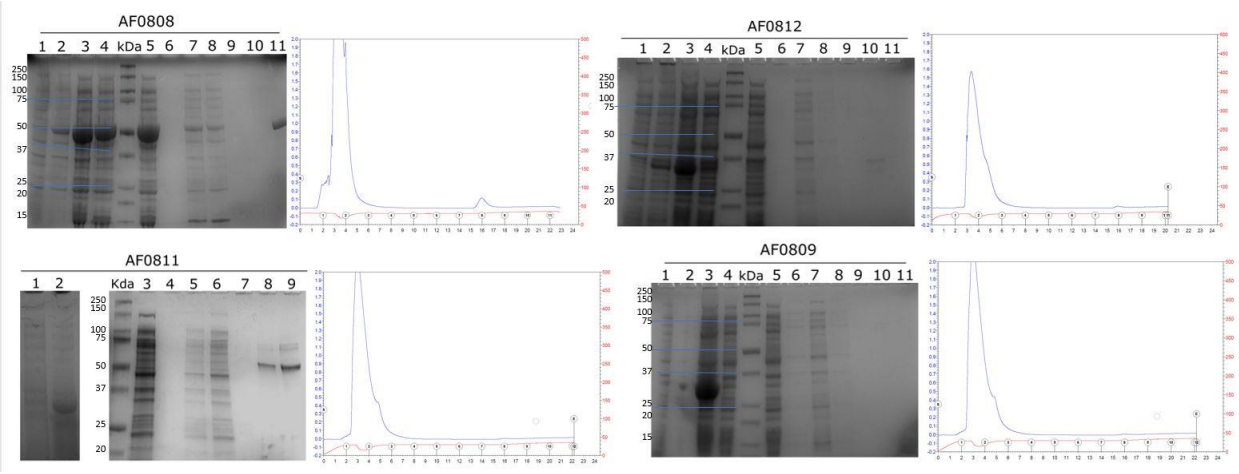

Figure 10 SDS-PAGE gels of samples and corresponding purification chromatograms of AF0808 (a.), AF0812 (b.), AF0811 (c.), and AF0809 (d.). Where lanes 1 and 2 correspond to cultures before (1) and after (2) induction with IPTG. Lanes 3 and 4 for AF0808, AF0812, and AF0809 correspond to the crude and clear lysate of the samples of induced cultures. Lanes 5 for AF0808, AF0812, and AF0809 and lane 3 for AF0811 correspond to the filtered lysate. Lanes 6, 7, and 8 of AF0808 and lanes 4, 5, and 6 of AF0811 correspond to fractions 1, 2, and 3 from the purifications of the proteins using an IMAC column. Lanes 6, 7, and 8 for AF0812 and AF0809 correspond to fractions 2, 3, and 4. **a.)** Lanes 9, 10, and 11 on the gel for AF0808 correspond to fractions 7, 8, and 9, where fraction 9 contains the target protein. **b.)** Lanes 9, 10, and 11 for AF0812 correspond to fractions 8, 9, and 10, where fraction 9 contains the target protein. **c.)** Lanes 7, 8, and 9 on the get for AF0811 correspond to fraction 8, fraction 9 concentrated, and fractions 8 and 9 combined and concentrated, where the concentrated fractions of just fraction 9 and 8 and 9 contain purified proteins. **d.)** Lanes 9, 10, and 11 of the gel for AF0809 correspond to fraction 9, fraction 9 concentrated, and fractions 8 and 9 combined and concentrated, respectively.

3.3.6 Gel Filtration of Purified Proteins

To separate and further purify the proteins purified using IMAC, the proteins obtained from cultures of clones containing genes for AF0808, AF0811, and AF0812 were all further analyzed using gel filtration to isolate target proteins and determine the size through a gel filtration column. AF0808 clones had the most significant amount of purified proteins. The chromatogram from the size exclusion showed three separations of proteins (**Figure 11**). When the contents of the fractions from the gel filtration were run on SDS-PAGE gel electrophoresis, it could be seen that the different proteins were of the same size and similar in size to the expected the target protein, a glycolate oxidase subunit of the putative LDH complex. All fractions appear to contain a protein of near 50 kDa in size based on the comparison to the protein standard used.

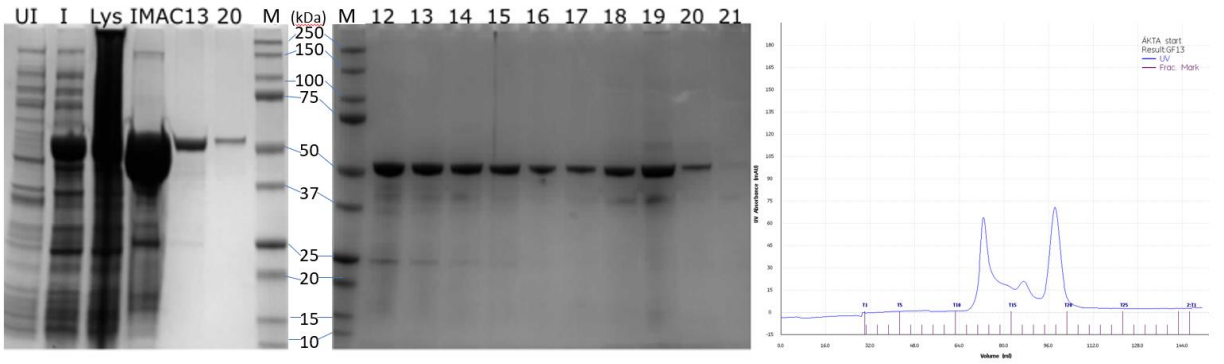

Figure 11 a.)SDS-PAGE gel of AF0808 clones through the process of growth, protein expression, purification and size exclusion. **b.)** SDS-PAGE gel from fractions after size exclusion **c.)** Chromatogram from size exclusion through gel filtration

Less protein was purified from AF0811 and the size of the purified proteins did not reflect that expected of the target protein. However, when two apparent purified proteins were separated using size exclusion, the size of the filtered protein was significantly smaller than the two proteins loaded, as seen on the bands from fractions 22 and 23 in the SDS-PAGE gel (**Figure 12**). Both bands fall between 25 and 37 kDa in size based on the comparison to the protein standard. There is also a lack of protein found in the SDS-PAGE gel that was indicated to be present in fractions 12 and 13 on the chromatogram.

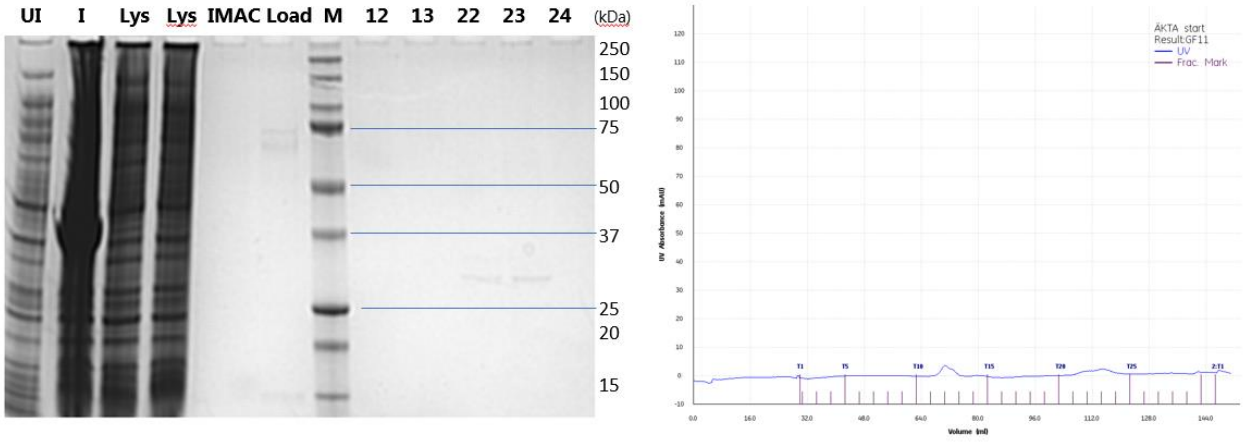

Figure 12 a.)SDS-PAGE gel of AF0811 clones through the process of growth, protein expression, purification and size exclusion. **b.)** Chromatogram from size exclusion through gel filtration

Two proteins were separated from the purified proteins of AF0812 clones, as seen by the two distinct peaks in the size exclusion chromatogram (**Figure 13**). The size exclusion shows that the

two proteins separated are about 34 and 30 kDa in size, based on the comparison to the Dual Color standard used in the SDS-PAGE gel electrophoresis.

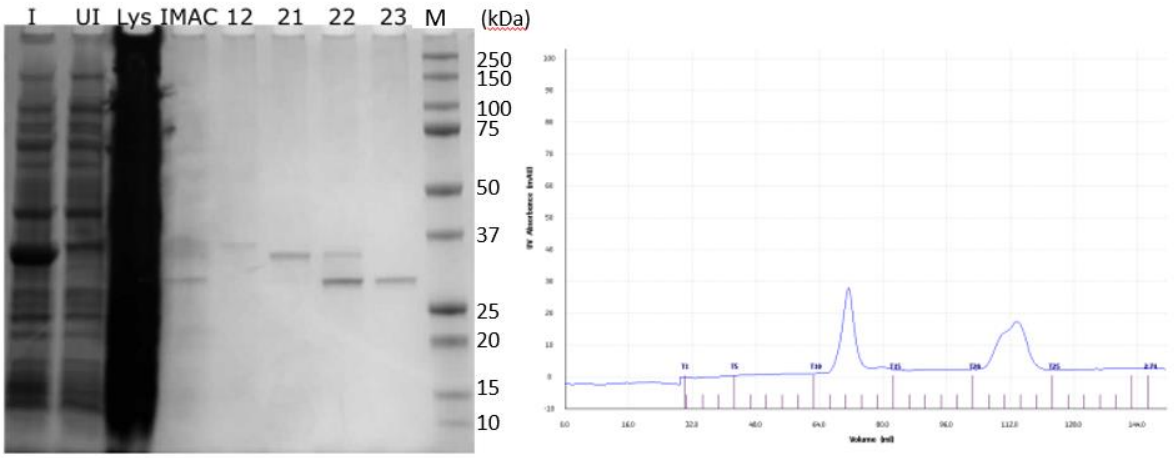

Figure 13 a.)SDS-PAGE gel of AF0812 clones through the process of growth, protein expression, purification and size exclusion. **b.)** Chromatogram from size exclusion through gel filtration

3.3.7 Circular Dichroism

When exchanging buffers for CD, the concentration of proteins measured after what remained from the overnight dialysis was too low to be read, so buffer exchange was repeated with remaining protein aliquots using the gel filtration column on the AKTÄ START. This second exchange was successful according to the Quantus, however the protein samples need to be concentrated to a high enough concentration for CD. The concentration reads on the Quantus were much higher than when measure of the NanoDrop or Direct Detect Spectrophotmeter.

Results from the circular dichroism scan indicated that the melting temperature of AF0808, the glycolate oxidase subunit, is near 82 °C based on the peak of the first derivative graph from the melting curve. The two curves of the CD scan at 20 °C and 95 °C vary, of which the curve of the 20 °C scan follows the known curves of proteins dominated by alpha helices, but also contains beta sheets and random coiling (**Figure 14**) (Greenfield and Fasman, 1969).

, h

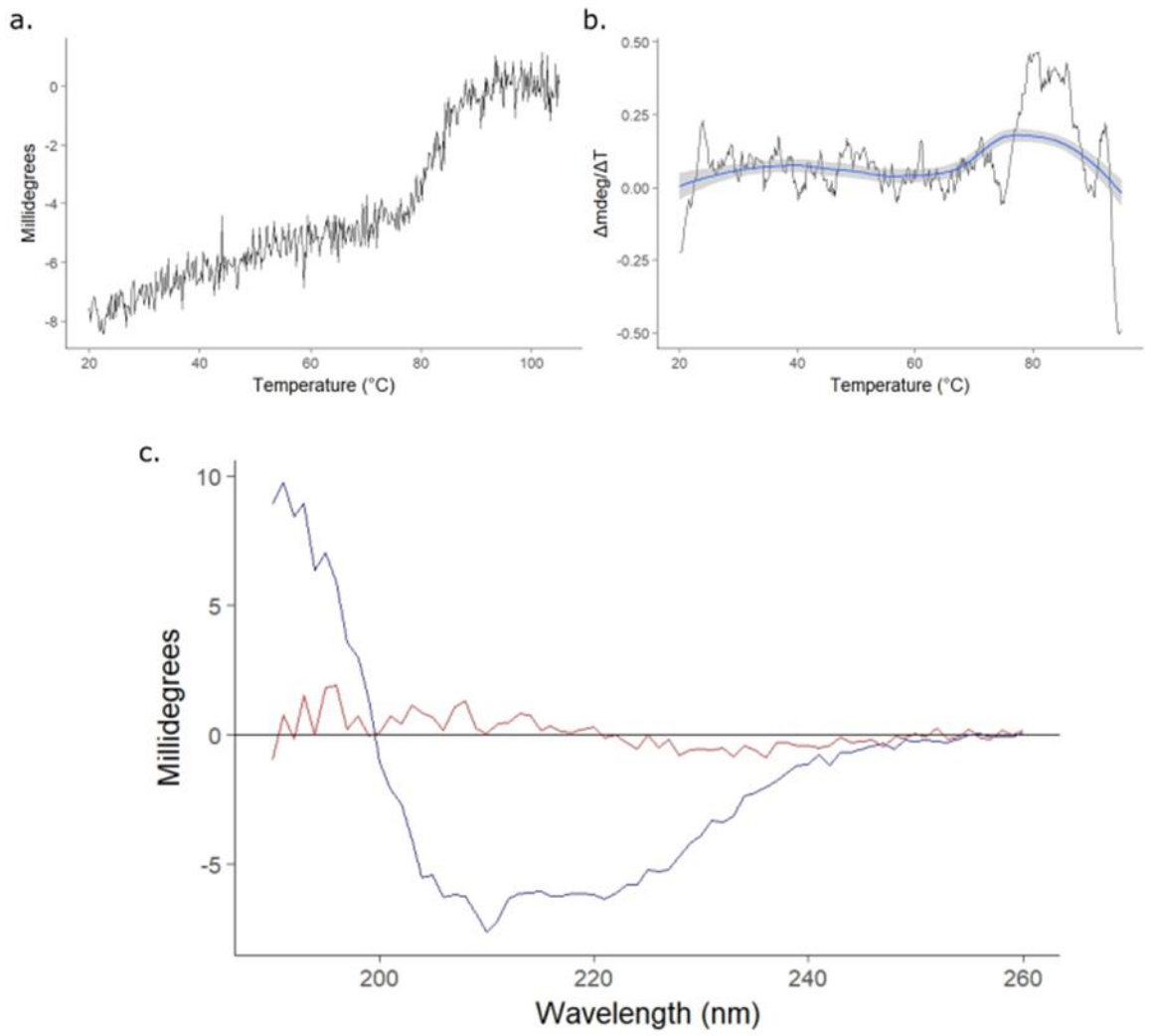

Figure 14 CD results for AF0808 with the temperature curve (a.) and the first derivative temperature curve (b.) and the CD scan data from 20 °C (blue) and 95 °C (red) from a wavelength of 190nm to 260nm.

4.0 Discussion

4.1 Sulfate Reduction

The purpose of measuring the surface layer in comparison to the entire slurry was to identify if DSR was primarily occurring on the outer surface or throughout the chimney wall. The extreme chemical and temperature gradients that occur within centimeters are characteristic of

hydrothermal vent chimneys and form small layers of micro-environments (Tivey, 1995). These steep gradients create favorable environments for certain organisms to grow. Hyperthermophiles that reduce sulfate typically have an optimal temperature for life at around 80 °C (Hartzell and Reed, 2006). This optimal temperature usually falls in the chimney wall where the hydrothermal fluids begin cooling as they mix with the sub-zero seawater (Tivey, 1995). The comparison of SRR between the full sample and the outer layer of the chimney could indicate the location where DSR is primarily occurring. This could give beneficial information for sampling in future research, as well as describe the gradients within the chimney wall in more detail. By measuring SRR of samples that had the addition of *Archaeoglobus* enrichment media and synthetic seawater, the aim was to see if enrichment for *Archaeoglobus* would have an effect on the SRR and give insight to limiting factors and possible competition.

Unfortunately, the sulfate reduction rates measured were extremely low and in less than half the samples. In comparison, Frank et al. (2013) found SRR in hydrothermal chimneys from 15.7 nmol g^{-1} day^{-1} to 2670 nmol g^{-1} day^{-1}. The rates found in this study were just about the detection limit and likely could easily fall below the detection limit given different approaches to the data analysis. There are several reasons why the rates may not have been found in all the samples. The lack of sulfate reduction rates found in the other samples from GS18-ROV22-ROCa and GS18-ROV22-ROCc might indicate the small amounts of microbial activity of SRPs present in the sample, including sulfur reducing archaea. The extremely low concentrations of DNA that were yielded in DNA extractions from the same slurry samples contribute to the argument that there could have been very little microbial activity in these samples.

It is possible that the samples were taken from a chimney or part of a chimney that was too hot for much life. SRR have been measured with an optimum rate at 91 °C in a hydrothermal chimney; however, we know chimney vent fluid can be around 350 °C and despite the cold surrounding seawater, it is possible that in this chimney segment seawater had not mixed enough with the vent fluids to cool to a temperature suitable for much life (Frank et al, 2013; Tivey, 1995, Jørgensen et al., 1992).

Another reason the sulfate reduction rates may have been so low and not have been found in almost all samples, is that organisms may have been using a different substrate as their terminal

electron acceptor. Although classified as sulfate reducers, many species can utilize other molecules as electron acceptors. Some sulfur reducing bacteria can utilize chromium (VI), manganese (IV), iron (III), and uranium (VI) as the only electron acceptors (Obraztsova and Tebo, 1998). It is possible that in these samples, despite the presence of sulfate, that the SRPs are using other electron acceptors, thereby leaving the tracer in oxidized form. This is supported by the fact that one sample gave detectable sulfate reduction rates, showing that sulfate reduction is possible in the sample but is not s dominating microbial process.

Other sources of error in lab work may have also resulted in the lack of measured sulfate reduction rates. Due to the constraints of time and material on the cruise, an anoxic environment was not maintained in the samples on the cruise. While some species of sulfate-reducers microbes can tolerate very little oxygen, or even use oxygen in the case of the sulfur reducing bacteria *Deculfovibrio oxyclinae*, many are strict anaerobes and could have died during the exposure to oxygen (Muyzer and Stams, 2008, Sigalevich and Cohen, 2000, Johnson et al., 1997). If this experiment were to be replicated, the use of a glove bag with constant nitrogen gas flow to maintain an anoxic environment for the samples may solve this issue. It would be important to immediately take the samples and place them in this environment. Another source of error may have come from the incubation time. The five-day incubation period may have been too short for the SRPs in the samples. Frank et. al (2013) incubated samples for 7 days under different temperatures. The five day incubation at 70 °C may have been conditions for slow growth and therefore the sulfate would have been reduced more slowly.

The samples collected strongly had the characteristic smell of hydrogen sulfide, the product of sulfate reduction, which led to the prediction that the samples were good candidates for environments with possibly high sulfate reduction rates (Rabus et al., 2013). However, it is possible that despite the high concentrations of hydrogen sulfide, that instead it was sourced from the vent fluid. The potency of the sample also lead to the hypothesis of high SRR due to possible high sulfate concentrations, however, high sulfate concentrations are not indicative of high sulfate reduction rates. In fact, Habicht et al. (2005) tested sulfate reduction rates with low sulfate concentrations in a chemostat experiment and limiting factors of sulfate reduction and found that low sulfate concentrations resulted in higher cell-specific sulfate reduction rates. It was also found that the sulfate concentrations impact which substrate is limiting. The shift in

metabolic pathways is hypothesized because when sulfate concentrations are low, the uptake of sulfate requires more energy. It was found here at low concentrations that sulfate is, therefore, not the limiting factor for sulfate reduction, only for growth and isotope fractionation. This gives supports that despite possible high concentrations of sulfur in the samples, sulfur reduction rates were low.

The low sulfate reduction rates found is reflected by similarly low relative abundance of sulfate reducers. Based on the low concentrations of DNA extracted from both slurries of GS18-ROV22-ROC, it is also likely that there is also a low total abundance of SRPs. There were no sulfate reducing archaea found in either sample from GS18-ROV22-ROCc; however it is likely the sulfate reduction could therefore be done by a sulfate reducing *Thermodesulfobacteriaceae* and *Desulfohalobiaceae*, as both sulfate reducing bacteria were found in the overall community of GS18-ROV22-ROCc. The low abundance of SRPs is not unexpected in this environment, as it was modelled by (Dahle et al., 2015) that the relative abundance of sulfate reducers was never over 7% at LCVF. It is, therefore, likely that sulfate reduction is occurring in sample by sulfate reducers, however at minute amounts due to the low abundance of SRPs. The fact that the only sample types that did not show SRR were those enriched with *Archaeoglobus* medium supports the community analysis data. Similarly, the Fark et al. (2013) study also showed a lack of presence of *Archaeoglobus* in the chimney samples collected, despite the high rates of sulfate reduction found. Overall, It is unlikely *Archaeoglobus* species are active in this section of chimney.

4.3 Cloning

One of the aims of this study was to identify if the lactate permease and putative lactate dehydrogenase (LDH) genes produce proteins that interact and encode for an oligomeric protein complex, as described as a possible interaction by Hocking et al. (2014). In order to test for the complex, information about the proteins needed to be gathered. The pI was crucial for determining the pH of the protein purification buffers in order to maintain protein stability. The size parameters of the proteins allowed for analysis on both Agarose and SDS-PAGE gels when using gel electrophoresis for DNA and proteins.

Unfortunately, not all target proteins were able to be expressed or produced as soluble proteins and it was, therefore, not possible to get a large breadth of knowledge on the putative LDH complex and test for complex forming proteins. Despite not being able to test protein interactions, more insight to the individual proteins was obtained, as well as details regarding the methods of producing and purifying these proteins.

4.3.1 Gibson Assembly® and Transformations

The genetic insert of AF0810, made from the ORF for the predicted coding region of the putative LDH complex, was not able to be amplified in PCR in order to be assembled into the pET-21a(+) vectors. There a couple reasons why this may have been unsuccessful. The first reason would be the design of the primers. The overlap of sequences was 40 base pairs (bp), of which it is recommended that 15 to 40 bp are used in overlap, so therefore the length of the overlap should not have been the issue in lack of amplification (SGI-DNA, 2018). It is, however, possible that in the homologous regions the design may have contained secondary structures that could have inhibited annealing (OpenWetWare, 2015). The second reason could be that the protocol used for the PCR reaction was not optimal for amplification of the insert. The large difference in annealing temperatures of the two primers may have caused only one primer to function, and therefore amplification would not occur. Although the annealing temperature was increased in the second attempt, it may have not been increased enough. A higher annealing temperature may have resulted in more successful amplification. Contributors of OpenWetWare (2015) suggest using primers with a minimum melting temperature of 72 °C for the primers, which was not the case for the primers of AF0810.

The assembled and purified plasmids were stored in stock at -20 °C, which allows for further testing on protein expression from these plasmids. Likewise, the confirmation that the inserts can be amplified and assembled into the pET-21a(+) vectors with the designed primers is beneficial for future studies. Repeated PCR amplifications of inserts using the designed primers, as well as additional primers for assembling multiple inserts into a single vector, would be advantageous for co-expression studies. The successful transformation of the plasmids into expression vectors allows for a pipeline of studying these genes from *A. fulgidus.* By testing the righteous

transformations, all purified plasmids, except for those containing AF0809can be transformed into competent cells in less time.

4.3.2 Protein production

Protein production was successful for four of the six cultures of clones from this study (**Figure)**. Despite multiple trials for expression, proteins were not produced in AF0806 and AF0807 clones. In the first growth trial of AF0806 clones, it was observed that absorbance of the culture decreased after induction of expression with IPTG. It is likely the decrease in absorbance indicates that the induction of expression of the proteins correlating to these genes results in cell death of the BL21-Codon Plus (DE3)-RIL cells (Rosano and Ceccarelli, 2014). It has been seen that some membrane proteins can result in cell death of BL21(DE3) cells (Miroux and Walker, 1996). The study done by Miroux and Walker (1996) indicates that the combination of IPTG and ampicillin might also contribute to a decrease in culture absorbance when expression of membrane proteins is induced. The ORF AF0806 encodes for a L-lactate permease, which would very likely be an integral membrane protein that would transfer lactate into the cell. Based on models from the ORF of AF0806 created in TMpred by Expasy (SIB Swiss Institue of Bioinformatics, Switzerlan), there are estimated 14 strong transmembrane helices within the protein sequence based on strongly preferred model (Appendix). This supports that AF0806 likely encodes for a transmembrane protein. Since AF0806 clones were also cultured in LB media containing ampicillin and induced with IPTG, this may have contributed to the decrease in optical density (Appendix). It is also possible that because AF0806 encodes for a transmembrane protein of an anaerobic species, it could not be produced in an aerobic environment. Likewise, the membrane structure of archaea and bacteria differ and that could have also been problematic for producing the archaeal membrane protein. Similar to AF0806 clones, growth of clones containing the AF0807 gene almost stopped after the addition of IPTG. This was seen by the diminished rate of increase of absorbance of the culture. This indicates that the cost of producing the protein is too high for the cells to continue investing in growth. Likewise, it is possible that for both proteins the rate of expression may have been too high to sustain cell growth in the first growth trials. In both cases, multiple trials were attempted with lengthening the incubation time

and lowering the incubation temperature. Both cases resulted in cell survival; however, there was still no production of protein. Despite unsuccessful protein production, it is still possible that under very slow and stable growing conditions proteins may be able to be produced.

Clones containing AF0809 produced only insoluble proteins, despite the multiple trials with varying incubation conditions and varying concentrations of IPTG to induce for expression. It is possible that this enzyme cannot be produced as a soluble protein when expressed alone and may need to be co-expressed. This supports the hypothesis by Hocking et al. (2014) of a lactate dehydrogenase complex, containing proteins from AF0808, AF0809, AF0810, and AF0812, where the enzymes function together. It could also be possible that the cellular localization of this putative heterodisulfide reductase is in the membrane. Since *A. fulgidus* can use L-lactate and D-lactate as a source of carbon and provide electrons to the dissimilatory sulfate reduction pathway for energy, these lactate dehydrogenase proteins are present to oxidize and transfer electrons within the cells (Reed and Hartzell, 1999, Stetter, 1988). The D-lactate dehydrogenase in *A. fulgidus* was found to be an integral membrane protein (Pagala et al., 2002). So, it is therefore likely that the protein associated with AF0809 could be a membrane associated or integral membrane protein, as suggested by Pagala et al. (2002) that the two lactate dehydrogenases in *A. fulgidus* are associated with the membrane because of their part in anaerobic respiration and DSR. A third reason for the insolubility might not be the location in the membrane, but that the protein is forming inclusion bodies, or highly aggregated and often cytoplasmic proteins that are common in high-expression in *E. coli* (Palmer and Wingfield, 2012). Often recombinant proteins, or proteins cloned into vectors for expression, aggregate in response to stress when induced for high levels of expression (Sørensen and Mortensen, 2005). Kim and Lee (2008) highlight the difficulties of producing hyperthermophilic archaeal proteins in *E.coli* and research ways to reduce the inclusion body formation. A fusion tag may be beneficial to add to the insert to help enhance the solubility of the proteins (Kim and Lee, 2008).

4.3.3 Glycolate Oxidase Subunit, AF0808

The amount of protein produced by AF0808 clones was substantial enough for further analysis using circular dichroism. The melting temperature found for this protein is characteristic of thermophiles; however, it is lower than for other proteins described in *A. fulgidus* (Langelandsvik et al., 1997, Vadas et al., 1999, Johnsen et al., 2003). The temperature range where unfolding began was in the range that *A. fulgidus* had been previously reported for optimum activity (ibid.). This also gives support for the hypothesis that the protein belongs to a protein complex, which would increase thermostability.

Another factor to consider with the results is the inconsistencies with the concentration measurements. It is likely the Quantus overestimates concentrations when following the protein concentration protocol because of the similarly lower readings given from NanoDrop and Direct Detect. The low concentration of purified protein run on the CD may have affected the read, and curves may not have been as representative as they could have been.

5.3.4 Suggestions for Further Studies

In future work, the first suggestion would be review and possibly design new primers for AF0810, despite there being no error found in the primer design. Given more time for the study, it would have been optimal to run more PCR trials with higher annealing temperatures.

For the remaining genes studied, and if successful AF0810 inserts are amplified, it might be beneficial to combine multiple genetic inserts into the pET-21a(+) vectors as possible with Gibson Assembly®. With Gibson Assembly®, multiple inserts can be cloned into one vector, up a total of several hundred kilobases in length, and transformed into *E. coli* in a single reaction (Gibson et al., 2009).This would allow for co-expression of genes to be done very simply in *E. coli*. As with the case of AF0809, it is possible that expression of insoluble proteins may be more likely to be soluble if the proteins are produced with the other complex forming members. However, if this method were to be used, it would not be advisable to insert AF0806 or AF0807 into the vectors due to the observed cell death of the BL21-Codon Plus (DE3)-RIL cells. Another option for obtaining soluble protein with AF0809 would be to adapt and modify the protocol

designed by Palmer and Wingfield (2012) using a guanidine·HCl buffer to help solubilize and unfold the protein during extractions.

To possibly produce proteins from clones of AF0806 and AF0807, a mutant host cell could also help with culture viability. Miroux and Walker (1996) used mutated C41(DE3) and double-mutated C43(DE3) cells in their study to produce viable cells and achieve protein expression in cells that had toxic over-expression for BL21(DE3) cells, where the double-mutated cells persisted the best with the toxic effects of over-expression of the membrane proteins.

To study the putative lactate dehydrogenase complex in *A. fulgidus*, another method could be to purify proteins from native cells instead expressing proteins in cloned cells. In a previous study, the genes encoding for the LDH complex were found to be up-regulated when enriched with sulfate (Hocking et al., 2014). It would be important to maintain anoxic conditions when studying native cells in order to preserve the stability of these proteins because of the anoxic characteristic of *A. fulgidus.*

5.0 Conclusion

The main purpose of this study was to better understand deep-sea hydrothermal vent ecosystems and the role that *Archaeoglobus* has as sulfate reducing archaea. By using biochemical, geochemical, and cultivation methods, this was achieved through two parts.

The first part of this study explored the sulfate reduction process in an environmental sample by following the sulfate reduction rates using radioactive isotopic tracers. Sulfate reduction rates were only found in one third of the samples taken, and were extremely low. The environmental samples collected from an active black smoker chimney from LCVF were also analyzed for community structure and relative abundance of species was determined for the outer portion of the chimney. The low yield from DNA extractions of the rock slurries inhibited extensive research on the community; however, with information given it was evident that *Archaeoglobus* were not present in the sample. This was supported by the lack of sulfate reduction rates found in any sample containing *Archaeoglobus* media. The DNA found of other thermophilic SRPs,

provide support to small amounts of sulfate reduction occurring in the chimney and which microbes may be responsible for reducing the sulfate.

The results from the sulfate reduction rate measurements emphasize the limitations to sampling in deep-sea hydrothermal vent systems. It is often time not until much after sampling that results can be seen and, therefore, it is very difficult to obtain good samples. In this case, the chimney fragment may have been from a part of the chimney that was too cool for *Archaeoglobus* to establish a community. Another limitation to this portion of the study was lack of previous experience with the geochemical methods of measuring sulfate reduction rates. Incubation times were difficult estimate and the conditions were fixed based on the shared space. The amount of samples taken was limited due to time and space constraints on the research cruise. However, despite the limitations, the study was valuable and given the information gathered, it would be advisable in future studies to maintain slurries in anaerobic environments as well as repeat the process with multiple chimney fragment samples from different parts of the chimney.

The second part of this study was an intracellular look into the dissimilatory sulfate reduction pathway in *A. fulgidus.* The putative LDH complex and related proteins were studied using methods in molecular and microbiology. Of the seven target proteins hypothesized to be in the complex or in association to it, three of the proteins belonging to the putative LDH complex were purified, with one remaining one expressed, but not purified. The glycolate oxidase subunit was produced in high enough concentrations to be studied for secondary structure and melting temperature. The results of this confirmed that the protein was thermostable and resembled the structure of other lactate dehydrogenases studied. Although the proteins were not all produced and purified and interactions between them able to be tested, insight was gained on the nature of the proteins. By producing some components of the putative LDH complex, the evidence towards the complex existing and playing an integral role in cellular metabolism is increased. The results also confirmed the existence of formerly hypothetical subunits for the complex. By supporting this hypothesis, a greater understanding of the cellular components needed to perform dissimilatory sulfate reduction is obtained.

Time was a major limitation for the second part of this overall study. Protein production and purification can be a process that involves a large amount of trial and error, as was in this case.

Given more time, production could have possibly been achieved for more target proteins by testing different growth conditions and lysing methods, as well as attempts of co-expression in one vector which would entail starting from Gibson cloning and creating a new expression vector with multiple genes of interest. However, to have produced three soluble proteins and expressed one other in the time given, the study was very fruitful as protein production can be very challenging.

Overall, this study provided a better understanding of the dissimilatory sulfate reducing archaea, *Archaeoglobus,* and the role they have in the deep-sea hydrothermal vent ecosystem in black smoker chimneys. The study also provided many opportunities to gain laboratory skills through biochemical, geochemical, molecular, and microbiological methods. Despite not having completely reaching the aims of the study, a greater insight was gained on DSR and sulfate reduction from sulfate reducers in black smoker chimneys through both parts of this study, as well as a more concrete understanding of the putative LDH complex and the role it likely has in energy conservation in *Archaeoglobus fulgidus*.

6.0 References

ACHENBACH-RICHTER, L., STETTER, K. O. & WOESE, C. R. 1987. A possible biochemical missing link among archaebacteria. *Nature,* 327**,** 348.

BAROSS, J. A., LILLEY, M. D. & GORDON, L. I. 1982. Is the CH4, H2 and CO venting from submarine hydrothermal systems produced by thermophilic bacteria? *Nature,* 298**,** 366.

CARSTENS, C., BONNARDEL, J., ALLEN, R. & WAESCHE, A. 2001. BL21-Codon-Plus cells correct expression problems caused by codon bias. *Strategies (Stratagene),* 14**,** 50-51.

CELIE, P. H. N., PARRET, A. H. A. & PERRAKIS, A. 2016. Recombinant cloning strategies for protein expression. *Current Opinion in Structural Biology,* 38**,** 145-154.

OPENWETWARE CONTRIBUTORS. 2015. *Janet B. Matsen: Guide to Gibson Assembly* [Online]. OpenWetWare. Accessed 13 March 2019. <https://openwetware.org/wiki/Janet_B._Matsen:Guide_to_Gibson_Assembly>

CORLISS, J. B., DYMOND, J., GORDON, L. I., EDMOND, J. M., VON HERZEN, R. P., BALLARD, R. D., GREEN, K., WILLIAMS, D., BAINBRIDGE, A. & CRANE, K. 1979. Submarine thermal springs on the Galapagos Rift. *Science,* 203**,** 1073-1083.

CRANE, K. & NORMARK, W. R. 1977. Hydrothermal activity and crestal structure of the East Pacific Rise at 21° N. *Journal of Geophysical Research,* 82**,** 5336-5348.

DAHLE, H., ØKLAND, I., THORSETH, I. H., PEDERESEN, R. B. & STEEN, I. H. 2015. Energy landscapes shape microbial communities in hydrothermal systems on the Arctic Mid-Ocean Ridge. *The ISME journal,* 9**,** 1593.

FOSSING, H. & JØRGENSEN, B. B. 1989. Measurement of bacterial sulfate reduction in sediments: Evaluation of a single-step chromium reduction method. *Biogeochemistry,* 8**,** 205-222.

FRANK, K. L., ROGERS, D. R., OLINS, H. C., VIDOUDEZ, C. & GIRGUIS, P. R. 2013. Characterizing the distribution and rates of microbial sulfate reduction at Middle Valley hydrothermal vents. *The ISME journal,* 7**,** 1391.

GARVIE, E. I. 1980. Bacterial lactate dehydrogenases. *Microbiological reviews,* 44**,** 106.

GIBSON, D. G., YOUNG, L., CHUANG, R.-Y., VENTER, J. C., HUTCHISON III, C. A. & SMITH, H. O. 2009. Enzymatic assembly of DNA molecules up to several hundred kilobases. *Nature Methods,* 6**,** 343.

GREENFIELD, N. J. & FASMAN, G. D. 1969. Computed circular dichroism spectra for the evaluation of protein conformation. *Biochemistry,* 8**,** 4108-4116.

HABICHT, K. S., SALLING, L., THAMDRUP, B. & CANFIELD, D. E. 2005. Effect of low sulfate concentrations on lactate oxidation and isotope fractionation during sulfate reduction by Archaeoglobus fulgidus strain Z. *Applied and Environmental Microbiology,* 71**,** 3770-7.

HARMSEN, H., PRIEUR, D. & JEANTHON, C. 1997. Distribution of microorganisms in deep-sea hydrothermal vent chimneys investigated by whole-cell hybridization and enrichment culture of thermophilic subpopulations. *Applied and Environmental Microbiology,* 63**,** 2876-2883.

HARTZELL, P. & REED, D. W. 2006. The genus Archaeoglobus. *The Prokaryotes: Volume 3: Archaea. Bacteria: Firmicutes, Actinomycetes,* 3, 82-100.

HOCKING, W. P., ROALKVAM, I., MAGNUSSEN, C., STOKKE, R. & STEEN, I. H. 2015. Assessment of the Carbon Monoxide Metabolism of the Hyperthermophilic Sulfate-Reducing Archaeon Archaeoglobus fulgidus VC-16 by Comparative Transcriptome Analyses. *Archaea,* 2015**,** 235384.

HOCKING, W. P., STOKKE, R., ROALKVAM, I. & STEEN, I. H. 2014. Identification of key components in the energy metabolism of the hyperthermophilic sulfate-reducing archaeon Archaeoglobus fulgidus by transcriptome analyses. *Frontiers in Microbiology,* 5**,** 95.

HUBER, H., JANNASCH, H., RACHEL, R., FUCHS, T. & STETTER, K. O. 1997. Archaeoglobus veneficus sp. nov., a novel facultative chemolithoautotrophic hyperthermophilic sulfite reducer, isolated from abyssal black smokers. *Systematic and Applied Microbiology,* 20**,** 374-380.

JAESCHKE, A., JØRGENSEN, S. L., BERNASCONI, S. M., PEDERSEN, R. B., THORSETH, I. H. & FRÜH-GREEN, G. L. 2012. Microbial diversity of Loki's Castle black smokers at the Arctic Mid-Ocean Ridge. *Geobiology,* 10**,** 548-561.

JANNASCH, H. W. & WIRSEN, C. O. 1979. Chemosynthetic Primary Production at East Pacific Sea Floor Spreading Centers. *BioScience,* 29**,** 592-598.

JOHNSEN, U., HANSEN, T. & SCHÖNHEIT, P. 2003. Comparative Analysis of Pyruvate Kinases from the Hyperthermophilic Archaea Archaeoglobus fulgidus, Aeropyrum pernix, and Pyrobaculum aerophilum and the Hyperthermophilic Bacterium Thermotoga maritima: unusual regulatory properties in hyperthemophilic archaea. *Journal of Biological Chemistry,* 278**,** 25417-25427.

JOHNSON, M. S., ZHULIN, I. B., GAPUZAN, M. E. & TAYLOR, B. L. 1997. Oxygen-dependent growth of the obligate anaerobe Desulfovibrio vulgaris Hildenborough. *Journal of Bacteriology,* 179**,** 5598-5601.

JØRGENSEN, B. B., ISAKSEN, M. F. & JANNASCH, H. W. 1992. Bacterial Sulfate Reduction Above 100°C in Deep-Sea Hydrothermal Vent Sediments. *Science,* 258**,** 1756-1757.

KALLMEYER, J., FERDELMAN, T. G., WEBER, A., FOSSING, H. & JØRGENSEN, B. B. 2004. A cold chromium distillation procedure for radiolabeled sulfide applied to sulfate reduction measurements. *Limnology and Oceanography: Methods,* 2**,** 171-180.

KELLEY, D. S., BAROSS, J. A. A. & DELANEY, J. R. 2002. Volcanoes, Fluids, and Life at Mid-Ocean Ridge Spreading Centers. *Annual Review of Earth and Planetary Sciences,* 30**,** 385-491.

KELLEY, D. S., KARSON, J. A., BLACKMAN, D. K., FRÜH-GREEN, G. L., BUTTERFIELD, D. A., LILLEY, M. D., OLSON, E. J., SCHRENK, M. O., ROE, K. K., LEBON, G. T., RIVIZZIGNO, P. & THE, A. T. S. P. 2001. An off-axis hydrothermal vent field near the Mid-Atlantic Ridge at 30° N. *Nature,* 412**,** 145-149.

KELLY, S. M., JESS, T. J. & PRICE, N. C. 2005. How to study proteins by circular dichroism. *Biochimica et Biophysica Acta (BBA)-Proteins and Proteomics,* 1751**,** 119-139.

KIM, S. & LEE, S. B. 2008. Soluble expression of archaeal proteins in Escherichia coli by using fusion-partners. *Protein Expression and Purification,* 62**,** 116-119.

KLENK, H.-P., CLAYTON, R. A., TOMB, J.-F., WHITE, O., NELSON, K. E., KETCHUM, K. A., DODSON, R. J., GWINN, M., HICKEY, E. K. & PETERSON, J. D. 1998. Corrections: The complete genome sequence of the hyperthermophilic, sulphate-reducing archaeon Archaeoglobus fulgidus. *Nature,* 394**,** 101.

KONHAUSER, K. O. 2009. *Introduction to Geomicrobiology*, John Wiley & Sons.

LANGELANDSVIK, A. S., STEEN, I. H., BIRKELAND, N. K. & LIEN, T. 1997. Properties and primary structure of a thermostable L-malate dehydrogenase from Archaeoglobus fulgidus. *Archives of Microbiology,* 168**,** 59-67.

LASO-PÉREZ, R., KRUKENBERG, V., MUSAT, F. & WEGENER, G. 2018. Establishing anaerobic hydrocarbon-degrading enrichment cultures of microorganisms under strictly anoxic conditions. *Nature Protocols,* 13**,** 1310.

LONSDALE, P. 1977. Clustering of suspension-feeding macrobenthos near abyssal hydrothermal vents at oceanic spreading centers. *Deep Sea Research,* 24**,** 857-863.

MIROUX, B. & WALKER, J. E. 1996. Over-production of proteins in Escherichia coli: mutant hosts that allow synthesis of some membrane proteins and globular proteins at high levels. *Journal of MolecularBiology,* 260**,** 289-298.

MORI, K., MARUYAMA, A., URABE, T., SUZUKI, K. & HANADA, S. 2008. Archaeoglobus infectus sp. nov., a novel thermophilic, chemolithoheterotrophic archaeon isolated from a deep-sea rock collected at Suiyo Seamount, Izu-Bonin Arc, western Pacific Ocean. *International Journal of Systematic and Evolutionary Microbiology,* 58**,** 810-6.

MUNN, C. B. 2011. *Marine Microbiology: Ecology and Applications*, Garland Science.

MUYZER, G. & STAMS, A. J. M. 2008. The ecology and biotechnology of sulphate-reducing bacteria. *Nature Reviews Microbiology,* 6**,** 441.

NAKAGAWA, T., NAKAGAWA, S., INAGAKI, F., TAKAI, K. & HORIKOSHI, K. 2004. Phylogenetic diversity of sulfate-reducing prokaryotes in active deep-sea hydrothermal vent chimney structures. *FEMS Microbiology Letters,* 232**,** 145-152.

NEUBAUER, P., HOFMANN, K., HOLST, O., MATTIASSON, B. & KRUSCHKE, P. 1992. Maximizing the expression of a recombinant gene in Escherichia coli by manipulation of induction time using lactose as inducer. *Applied Microbiology and Biotechnology,* 36**,** 739-744.

OBRAZTSOVA, A. Y. & TEBO, B. M. 1998. Sulfate-reducing bacterium grows with Cr(VI), U(VI), Mn(IV), and Fe(III) as electron acceptors. *FEMS Microbiology Letters,* 162**,** 193-199.

PAGALA, V. R., PARK, J., REED, D. W. & HARTZELL, P. L. 2002. Cellular localization of D-lactate dehydrogenase and NADH oxidase from Archaeoglobus fulgidus. *Archaea,* 1**,** 95-104.

PALMER, I. & WINGFIELD, P. T. 2012. Preparation and extraction of insoluble (inclusion-body) proteins from Escherichia coli. *Current Protocols in Protein Science,* 70**,** 6.3. 1-6.3. 20.

PECK, H. D., JR. 1961. Enzymatic basis for assimilatory and dissimilatory sulfate reduction. *Journal of Bacteriology,* 82**,** 933-939.

PEDERSEN, R. B., RAPP, H. T., THORSETH, I. H., LILLEY, M. D., BARRIGA, F. J. A. S., BAUMBERGER, T., FLESLAND, K., FONSECA, R., FRÜH-GREEN, G. L. & JORGENSEN, S. L. 2010. Discovery of a black smoker vent field and vent fauna at the Arctic Mid-Ocean Ridge. *Nature Communications,* 1**,** 126.

PFENNIG, N., WIDDEL, F. & TRÜPER, H. G. 1981. The dissimilatory sulfate-reducing bacteria. *The Prokaryotes.* Springer.

POPE, B. & KENT, H. M. 1996. High efficiency 5 min transformation of Escherichia coli. *Nucleic Acids Research,* 24**,** 536-537.

POSTGATE, J. 1959. Sulphate reduction by bacteria. *Annual Reviews in Microbiology,* 13**,** 505-520.

RABUS, R., HANSEN, T. A. & WIDDEL, F. 2013. Dissimilatory sulfate-and sulfur-reducing prokaryotes. *The Prokaryotes: Prokaryotic Physiology and Biochemistry***,** 309-404.

RABUS, R., VENCESLAU, S. S., WOHLBRAND, L., VOORDOUW, G., WALL, J. D. & PEREIRA, I. A. 2015. A Post-Genomic View of the Ecophysiology, Catabolism and Biotechnological Relevance of Sulphate-Reducing Prokaryotes. *Advances in Microbial Physiology,* 66**,** 55-321.

RAMOS, A., KELLER, K., WALL, J. & PEREIRA, I. A. 2012. The membrane QmoABC complex interacts directly with the dissimilatory adenosine 5´-phosphosulfate reductase in sulfate reducing bacteria. *Frontiers in Microbiology,* 3.

REED, D. W. & HARTZELL, P. L. 1999. The Archaeoglobus fulgidus D-lactate dehydrogenase is a Zn2+ flavoprotein. *Journal of Bacteriology,* 181**,** 7580-7587.

RONA, P., KLINKHAMMER, G., NELSEN, T., TREFRY, J. & ELDERFIELD, H. 1986. Black smokers, massive sulphides and vent biota at the Mid-Atlantic Ridge. *Nature,* 321**,** 33.

ROSANO, G. L. & CECCARELLI, E. A. 2014. Recombinant protein expression in Escherichia coli: advances and challenges. *Frontiers in microbiology,* 5**,** 172.

SCOTT, R. B., RONA, P. A., MCGREGOR, B. A. & SCOTT, M. R. 1974. The TAG hydrothermal field. *Nature,* 251**,** 301-302.

SIGALEVICH, P. & COHEN, Y. 2000. Oxygen-Dependent Growth of the Sulfate-Reducing Bacterium Desulfovibrio oxyclinae in Coculture with Marinobacter sp. Strain MB in an Aerated Sulfate-Depleted Chemostat. *Applied and Environmental Microbiology, 66*(11), 5019-5023.

SØRENSEN, H. P. & MORTENSEN, K. K. 2005. Advanced genetic strategies for recombinant protein expression in Escherichia coli. *Journal of Biotechnology,* 115**,** 113-128.

STEINSBU, B. O., THORSETH, I. H., NAKAGAWA, S., INAGAKI, F., LEVER, M. A., ENGELEN, B., ØVREÅS, L. & PEDERSEN, R. B. 2010. Archaeoglobus sulfaticallidus sp. nov., a thermophilic and facultatively lithoautotrophic sulfate-reducer isolated from black rust exposed to hot ridge flank crustal fluids. *International Journal of Systematic and Evolutionary Microbiology,* 60**,** 2745-2752.

STETTER, K. O. 1988. Archaeoglobus fulgidus gen. nov., sp. nov.: a new taxon of extremely thermophilic archaebacteria. *Systematic and Applied Microbiology,* 10**,** 172-173.

STUDIER, F. W. & MOFFATT, B. A. 1986. Use of bacteriophage T7 RNA polymerase to direct selective high-level expression of cloned genes. *Journal of Molecular Biology,* 189**,** 113-130.

TIVEY, M. K. 1995. The influence of hydrothermal fluid composition and advection rates on black smoker chimney mineralogy: Insights from modeling transport and reaction. *Geochimica et Cosmochimica Acta,* 59**,** 1933-1949.

VADAS, A., MONBOUQUETTE, H. G., JOHNSON, E. & SCHRODER, I. 1999. Identification and characterization of a novel ferric reductase from the hyperthermophilic Archaeon Archaeoglobus fulgidus. *Journal of Bioogical Chemistry,* 274**,** 36715-21.

VAN DOVER, C. L. 1995. Ecology of mid-Atlantic ridge hydrothermal vents. *Geological Society, London, Special Publications,* 87**,** 257-294.

VON JAN, M., LAPIDUS, A., DEL RIO, T. G., COPELAND, A., TICE, H., CHENG, J. F., LUCAS, S., CHEN, F., NOLAN, M., GOODWIN, L., HAN, C., PITLUCK, S., LIOLIOS, K., IVANOVA, N., MAVROMATIS, K., OVCHINNIKOVA, G., CHERTKOV, O., PATI, A., CHEN, A., PALANIAPPAN, K., LAND, M., HAUSER, L., CHANG, Y. J., JEFFRIES, C. D., SAUNDERS, E., BRETTIN, T., DETTER, J. C., CHAIN, P., EICHINGER, K., HUBER, H., SPRING, S., ROHDE, M., GOKER, M., WIRTH, R., WOYKE, T., BRISTOW, J., EISEN, J. A., MARKOWITZ, V., HUGENHOLTZ, P., KYRPIDES, N. C. & KLENK, H. P. 2010. Complete genome sequence of Archaeoglobus profundus type strain (AV18). *Standards in Genomic Science,* 2**,** 327-46.

YAMAMOTO, M. & TAKAI, K. 2011. Sulfur metabolisms in epsilon-and gamma-Proteobacteria in deep-sea hydrothermal fields. *Frontiers in Microbiology,* 2**,** 192.

Appendix A

List of solutions and buffers

Gel Electrophoresis

1% Agarose gels
- 0.4g Agarose
- 40 mL 1X TAE buffer
  - 40 mM Tris Base
  - 20 mM Acetic Acid
  - 1 mM EDTA sodium salk dihydrate
- Microwaved covered until agarose dissolved
- Cooled
- 4 µl 1000x GelGreen Nucleic Acid
- Poured into mold, covered, and left to set

Cloning

LB agar plates
- 10 g/L NaCl
- 10 g/L tryptone
- 5 g/L yeast extract 20 g/L agar
- Brought to volume with deionized H2O
- Adjusted pH to 7.0 with 5 N NaOH
- Sterilized with autoclave
- Cooled to 55°C
- 50 µg/ml Ampicillin
- 50 µg/ml Chloramphenicol
- Poured ~25ml per plate

LB broth
- 10 g/L NaCl
- 10 g/L tryptone
- 5 g/L yeast extract
- Brought to volume with distilled water
- pH adjusted to 7.0 with 5 N NaOH
- sterilized
- 50 µg/ml Ampicillin
- 50 µg/ml Chloramphenicol

$^{35}SO_4^{2-}$ Incubations

25 wt% zinc acetate solution
- 50g of zinc acetate
- 200 ml of ultrapure water

$^{35}SO_4^{2-}$ tracer solution (37 MBq)

50% $^{35}SO_4^{2-}$ tracer
50% Milli-Q water

Cold Chromium Reduction

2N HCl
200 ml 30% HCl
800 ml milli-Q

6N HCl
600 ml 30% HCl
370 ml milli-Q

5% ZnAc
50 g zinc acetate
950 ml milli-Q

0.1M citric acid
19.2 g citric acid
1000 ml milli-Q
4 g NaOH (adjust to pH 4)

0.5M Na2S
6 g Na2¬S.9H2O
0 ml milli-Q

1M CrCl3 in 2N HCl
1000 g CrCl3.6H2O
640 ml 30% HCl + 3440 ml milli-Q

Protein Purification and Gel Filtration

HEPES Lysis Buffer:
50mM HEPES pH 7.5
300mM NaCl
10% Glycerol
0.25 mg/ml Lysozyme

HEPES Buffer A:
20mM HEPES pH 7.5
500mM NaCl
10mM Imidazol

HEPES Elution Buffer B:
20mM HEPES pH 7.5
500mM NaCl

550mM Imidazol

HEPES Size-exclusion Running Buffer:
20mM HEPES pH 7.5
300mM NaCl
1L
*degassed and filtered

HEPES Storage Buffer
20mM HEPES pH 7.5
300mM NaCl
2mM TCEP (reducing agent for disulphide bridges)
30% Glycerol (for safe storage at -20C)

Protocols

(MP Biomedicals, LLC, Santa Ana, CA, USA)

http://dmoserv3.whoi.edu/data_docs/IODP_347/FastDNA_Spin_Kit_for_Soil.pdf

NEB Gibson Assembly® Cloning Kit (New England BioLabs, Ipswich, MA, USA)

DpnI protocol:

1. In a total 10 µl reaction, mix 5–8 µl of PCR product with 1 µl of 10X Cutsmart and 1 µl (20 units) of DpnI.

2. Incubate at 37°C for 30 minutes.

3. Heat-inactivate DpnI by incubating at 80°C for 20 minutes.

Gibson Assembly Protocol:

1. Set up the following reaction on ice:

2. Incubate samples in a thermocycler at 50°C for 15 minutes when 2 or 3 fragments are being assembled or 60 minutes when 4-6 fragments are being assembled. Following incubation, store samples on ice or at –20°C for subsequent transformation.

3. Transform NEB 5-alpha Competent *E. coli* cells (provided with the kit) with 2 µl of the assembly reaction

Transformation Protocol

1. Thaw chemically competent cells on ice.

2. Add 2 µl of the chilled assembly product to the competent cells. Mix gently by pipetting up and down or by flicking the tube 4–5 times. Do not vortex.

3. Place the mixture on ice for 30 minutes. Do not mix.

4. Heat shock at 42°C for 30 seconds. Do not mix.

5. Transfer tubes to ice for 2 minutes.

6. Add 950 µl of room-temperature SOC media to the tube.

7. Incubate the tube at 37°C for 60 minutes. Shake vigorously (250 rpm) or rotate.

8. Warm selection plates to 37°C.

9. Spread 100 µl of the cells onto the selection plates. Use Amp plates for positive control sample.

10. Incubate overnight at 37°C.

https://www.neb.com/-/media/catalog/datacards-or-manuals/manuale5510.pdf

Monarch® Plasmid Miniprep Kit (New England BioLabs, Ipswich, MA, USA)

1. **Pellet 1–5 ml (not to exceed 15 OD units) bacterial culture by centrifugation for 30 seconds. Discard supernatant.**1.5 ml of culture is sufficient for most applications. Ensure cultures are not overgrown (12-16 hours is ideal).
2. **Resuspend pellet in 200 µl Plasmid Resuspension Buffer (B1) (pink).** Vortex or pipet to ensure cells are completely resuspended. There should be no visible clumps.
3. **Add 200 µl Plasmid Lysis Buffer (B2) (green), gently invert tube 5–6 times, and incubate at room temperature for 1 minute.** Color should change to dark pink, and solution will become transparent and viscous. Do not vortex.
4. **Add 400 µl of Plasmid Neutralization Buffer (B3) (yellow), gently invert tube until neutralized, and incubate at room temperature for 1 minute.** Sample is neutralized when color is uniformly yellow and precipitate forms. Do not vortex.
5. **Centrifuge lysate for 2–5 minutes.** For best results, and especially culture volumes > 1 ml, we recommend a 5 minute spin to ensure efficient RNA removal by RNase A. Pellet should be compact; spin longer if needed.

6. **Carefully transfer supernatant to the spin column and centrifuge for 1 minute. Discard flow-through.**
7. **Re-insert column in the collection tube and add 200 µl of Plasmid Wash Buffer 1. Centrifuge for 1 minute.** Discarding the flow-through is optional.
8. **Add 400 µl of Plasmid Wash Buffer 2 and centrifuge for 1 minute.**
9. **Transfer column to a clean 1.5 ml microfuge tube.** Use care to ensure that the tip of the column does not come into contact with the flow-through. If there is any doubt, re-spin the column for 1 minute.
10. **Add ≥ 30 µl DNA Elution Buffer to the center of the matrix. Wait for 1 minute, then spin for 1 minute to elute DNA.** Nuclease-free water (pH 7–8.5) can also be used to elute the DNA. Yield may slightly increase if a larger volume of DNA Elution Buffer is used, but the DNA will be less concentrated. For larger size DNA, (≥ 10 kb), heating the elution buffer to 50°C prior to use can improve yield.

https://www.neb.com/-/media/catalog/Datacards%20or%20Manuals/manualT1010.pdf

Quantas Flourometer DNA Concentration measurement protocol (Promega Corporation, Madison, WI, USA)

Prepare 1X TE buffer by diluting 20X TE Buffer (pH 7.5) to 1X with nuclease-free water. For example, combine 200µl of 20X TE Buffer and 3,800µl of nuclease-free water to prepare 4ml of 1X TE buffer.

2. Prepare the QuantiFluor® Dye working solution with 1X TE buffer as follows. For example, to make a 1:400dilution, combine 10µl of QuantiFluor® Dye with 3,990µl of 1X TE buffer, and mix.

3. Prepare the nucleic acid standard in a 0.5ml PCR tube. Use the volume of supplied standard

Promega Corporation · 2800 Woods Hollow Road · Madison, WI 53711-5399 USA · Toll Free in USA 800-356-9526 · 608-274-4330 · Fax 608-277-2516 9

www.promega.com TM396 · Revised 12/18

4. Prepare the blank sample for the QuantiFluor® ONE dsDNA System by adding 200µl of QuantiFluor® ONE dsDNA Dye to a 0.5ml PCR tube. Prepare the blank sample for all other QuantiFluor® Systems by adding 200µl of QuantiFluor® Dye working solution prepared in Step 2 to a 0.5ml PCR tube.

5. For QuantiFluor® ONE dsDNA System, add 1µl of the standard to 200µl of QuantiFluor® ONE dsDNA Dye. For all other QuantiFluor® Systems, add standard prepared in Step 3 to 200µl of QuantiFluor® Dye working solution prepared in Step 2.

6. Mix three times by pipetting slowly. When using aerosol-resistant pipette tips, do not allow the pipette tip filter to get wet. Alternatively, vortex tubes at a high setting for 10 seconds.

7. Optional: Centrifuge tubes at 2,000 × g for 5–10 seconds to collect liquid at the bottom of the tube and remove any bubbles present.

8. Incubate tubes at room temperature for 5 minutes, protected from light.

Calibration Protocol

1. Select the desired QuantiFluor® Dye assay from the Protocol screen on the instrument. If this is the first time the protocol has been selected, the Calibration screen will automatically appear. Otherwise, after selecting the desired protocol, navigate to the Calibration screen.

2. Place the blank sample into the tube holder, and close the lid. Select “Read Blank”, and the fluorescence in relative fluorescence units (RFU) for the blank sample will be displayed on the screen.

3. Place the standard sample into the tube holder, and close the lid. Select “Read Std”, and the fluorescence in RFU for the standard sample will be displayed on the screen.

https://www.promega.com/-/media/files/resources/protocols/technical-manuals/101/quantus-fluorometer-operating-manual.pdf?la=en

BL21-CodonPlus Competent Cells Transformation Protocol

1. Thaw the competent cells on ice.
2. Gently mix the competent cells. Aliquot 100 µl of the competent cells into the appropriate number of prechilled 14-ml BD Falcon polypropylene round-bottom tubes. Prepare an additional 100-µl aliquot of cells for use as a transformation control.
3. Dilute XL10-Gold β-mercaptoethanol mix provided with this kit 1:10 with dH2O. Each 100-µl aliquot of cells requires 2 µl of diluted β-mercaptoethanol.
4. Add 2.0 µl of the 1:10 dilution of β-mercaptoethanol to each of the 100-µl aliquots of competent cells.
5. Swirl the contents of the tubes gently. Incubate the cells on ice for 10 minutes, swirling gently every 2 minutes.

6. Add 1–50 ng of expression plasmid DNA containing the gene of interest to each tube of cells and swirl gently.
7. Incubate the reactions on ice for 30 minutes.
8. Preheat SOC mediumin a 42°C water bath for use in step 11.
9. Heat-pulse each transformation reaction in a 42°C water bath for 20 seconds.
10. Incubate the reactions on ice for 2 minutes.
11. Add 0.9 ml of preheated (42°C) SOC medium to each transformation reaction and incubate the reactions at 37°C for 1 hour with shaking at 225–250 rpm.
12. Using a sterile spreader, spread ≤ 200 µl of the cells transformed with the experimental DNA onto LB agar plates that contain the appropriate antibiotic.

https://www.agilent.com/cs/library/usermanuals/public/230240.pdf

Appendix B

Measuring Primer concentrations

Primers were resuspended using UV treated milli-Q water in accordance to amount of nucleic acids given by the producer to obtain a concentration of 100μM. The concentrations were then diluted 1:10 and checked for accuracy by measuring the optical density at 260 nanometers (nm) using Cary300 spectrophotometer. The concentration was calculated with the following formula (Formula 2.1):

Formula 2.1 The formula to obtain concentration values using the optical density from a spectrophotometer and molecular weight.

$$concentration = \frac{optical\ density\ measured\ by\ Cary300\ \times 1000}{calculated\ molecular\ weight}$$

When the primer concentrations were either confirmed or corrected to be at a concentration of 100 μM, aliquots were taken and diluted to a concentration on 10 μM and stored at -20°C until use.

Appendix C

C.1 Scintillation Counts and SRR calculations

Table C.1 Measurements from scintillation counter reads and the overall value for counts per minute (CPMA) given in bold. Separated by distillation date with the background calculated for the sample types on each date in the bottom of the table. The detection limit for each sample type on each day was calculated using the background. With the porosity measurements from the two rocks, sulfate reduction rates were calculated for samples that had scintillation counts above the detection limit.

12-Dec	CPMA(co	[SO4]	SRR	13.nov	CPMA	[SO4]	16.nov	CPMA	[SO4]	SRR
blank	36			blank	23		c-seawater	36		
blank	35			blank	25		c-seawater	34		
blank	**35**			**blank**	**24**		**c-seawater**	**35**	**5,512**	0,201
a-seawater	36			c-media	25		c-seawater super	51380		
a-seawater	35			c-media	23		c-seawater super	51429		
a-seawater	**36**	**2,099**	0,142	**c-media**	**24**	**-6,606**	**c-seawater super**	**51404**	**51374,512**	
c-seawater	26			c-media supernantant	49968		c-seawater	49		
c-seawater	29			c-media supernantant	50070		c-seawater	50		
c-seawater	**27**	**-7,497**		**c-media supernantant**	**50019**		**c-seawater**	**49**	**19,512**	0,769
a-seawater no tracer control	24			c-media	26		c-seawater supernatent	47436		
a-seawater no tracer control	23			c-media	26		c-seawater supernatent	47439		
a-seawater no tracer control	**23**			**c-media**	**26**	**-4,606**	**c-seawater supernatent**	**47438**	**47408,512**	
a-seawater	25			c-media supernantant	82034		c-media	30		
a-seawater	24			c-media supernantant	82194		c-media	30		
a-seawater	**24**	**-9,901**		**c-media supernantant**	**82114**		**c-media**	**30**	**-1,183**	
c-media	21			c-seawater	23		c-media super	44597		
c-media	20			c-seawater	23		c-media super	44545		
c-media	**21**	**-14,176**		**c-seawater**	**23**	**-6,183**	**c-media super**	**44571**		
a-seawater tracer control	22			c-seawater supernatant	46211		a-seawater	32		
a-seawater tracer control	23			c-seawater supernatant	46124		a-seawater	35		
a-seawater tracer control	**22**			**c-seawater supernatant**	**46168**		**a-seawater**	**34**	**5,547**	0,422
a-seawater supernatant	59526			a-seawater	24		a-seawater supernatent	53025		
a-seawater supernatant	59538			a-seawater	25		a-seawater supernatent	53035		
a-seawater supernatant	**59514**	**59480,099**		**a-seawater**	**24**	**0,000**	**a-seawater supernatent**	**53030**	**53001,547**	
c-seawater supernatant	37121			a-seawater supernatant	69360		c-seawater tracer control	30		
c-seawater supernatant	37110			a-seawater supernatant	69323		c-seawater tracer control	27		
c-seawater supernatant	**37115**			**a-seawater supernatant**	**69341**		**c-seawater tracer control**	**29**		
a-seawater no tracer control supernatent	19			c-media tracer control	27		c-seawater tracer control super	57354		
a-seawater no tracer control supernatent	22			c-media tracer control	25		c-seawater tracer control super	57403		
a-seawater no tracer control supernatent	**21**			**c-media tracer control**	**26**		**c-seawater tracer control super**	**57378**		
a-seawater supernatant	56549			c-media tracer control supernatant	61023		c-seawater no tracer control	27		
a-seawater supernatant	56495			c-media tracer control supernatant	61038		c-seawater no tracer control	26		
a-seawater supernatant	**56521**			**c-media tracer control supernatant**	**61030**		**c-seawater no tracer control**	**27**		
c-media supernatant	40949			c-media no tracer control	30		c-seawater no tracer control supernatent	34		
c-media supernatant	40850			c-media no tracer control	33		c-seawater no tracer control supernatent	33		
c-media supernatant	**40899**			**c-media no tracer control**	**31**		**c-seawater no tracer control supernatent**	**33**		
a-seawater tracer control supernatant	77154			c-media no tracer control supernatant	24		blank	30		
a-seawater tracer control supernatant	77111			c-media no tracer control supernatant	23		blank	29		
a-seawater tracer control supernatant	**77133**			**c-media no tracer control supernatant**	**23**		**blank**	**29**		
a-seawater Bs		26,667				23,000			24,667	
c-media Bs		30,667				27,000			28,667	
c-seawater Bs		30,333				26,667			28,333	
detection limit a-seawater		33,901				24,000			28,453	
detection limit c-media		35,176				30,606			31,183	
detection limit c-seawater		34,497				29,183			29,488	
a-porosity	0,679									
c-porosity	0,315									

C.2 Culture Growth and Induction of Protein Expression

Table C.2 recorded OD(600nm) measurements of batch culture growths over time, inductions with IPTG occurred where highlighted.

time (minutes)	AF0806 (100ml, 1M IPTG)		AF0806 (100ml, 1M IPTG)		AF0807 (100ml, 1M IPTG)	AF0807 (100ml, 1M IPTG)	AF0808 (100ml, 1M IPTG)	AF0809 (100ml, 1M IPTG)	AF0809 (100ml, 1M IPTG)	AF0809 (100ml, 1 M IPTG)	AF0811 (100ml, 1M IPTG)	AF0812 (100ml, 1M IPTG)
0	0,08		0,08		0,13	0,143	0,144		0,13	0,09		
30						0,172	0,172					
45	0,22		0,22		0,29				0,26	0,14		
60						0,245	0,239					
75	0,4	0,56	0,45	0,52	0,52				0,45	0,21		
90						0,399	0,386					
100										0,28		
105						0,487	0,46					
115						0,522	0,506	0,47		0,33		
130										0,41		
135	0,55		0,54		0,89				0,84			
150						0,845	0,818					
165	0,52		0,56		1,01				1	0,72		
180						1,053	1,022					
185	0,52		0,6		1,1				1,12	0,79		
200										0,84		
210						1,197	1,175					
240						1,307	1,276					
		1,12		1,44				1,45				